Electronic Supplementary Information

Rare-earth element doped NiFe-MOFs as efficient and robust bifunctional electrocatalysts for both alkaline freshwater and seawater splitting

Jun Yang,‡[ab] Yong Shen,‡[a] Jiahui Xian,[a] Runan Xiang[a] and Guangqin Li*[a]

[a] MOE Laboratory of Bioinorganic and Synthetic Chemistry, GBRCE for Functional Molecular Engineering, Lehn Institute of Functional Materials, School of Chemistry, Sun Yat-Sen University, Guangzhou 510006, China
E-mail: liguangqin@mail.sysu.edu.cn
[b] School of Chemical Engineering, Guangdong University of Petrochemical Technology, Maoming 525000, China
‡ These authors contributed equally to this work.

Experimental Section

Materials

All chemicals were purchased from commercial sources and directly used without further purification. The nickel foam (NF) substrates (2.0 cm × 3.0 cm) were carefully cleaned with acetone, deionized water and absolute ethanol by ultrasonic treatment.

Synthesis of NiFe-MOF

Firstly, 1.0 mmol of $FeCl_2·4H_2O$ (98%) and 1.0 mmol of terephthalic acid (99%) were dissolved in a mixed solvent of 10.5 mL of N,N-dimethylformamide (DMF), 0.75 mL of absolute ethanol and 0.75 mL of deionized water. Subsequently, the obtained solution and a piece of NF were transferred into 25 mL of Teflon-lined autoclave and heated at 125 ºC for 12 h. After cooling, the self-supporting NiFe-MOF electrode was repeatedly washed with deionized water and then dried at 60 °C in a vacuum oven.

Synthesis of CeNiFe-MOF

Firstly, 1.0 mmol of $FeCl_2·4H_2O$ (98%), 1.0 mmol of terephthalic acid (99%) and 0.05 mmol of $Ce(NO_3)_3·6H_2O$ (99.95%) were dissolved in a mixed solvent of 10.5 mL of DMF, 0.75 mL of absolute ethanol and 0.75 mL of deionized water. Subsequently, the obtained solution and a piece of NF were transferred into 25 mL of Teflon-lined autoclave and heated at 125 ºC for 12 h. After cooling, the self-supporting CeNiFe-MOF electrode was repeatedly washed with deionized water and then dried at 60 °C in a vacuum oven. Other CeNiFe-MOF samples with different Ce content were also prepared in the same way by adding 0.01 and 0.1 mmol of $Ce(NO_3)_3·6H_2O$, respectively.

Synthesis of YNiFe-MOF and LaNiFe-MOF

The self-supporting YNiFe-MOF and LaNiFe-MOF electrodes were prepared in the same way by using $Y(NO_3)_3·6H_2O$ (99.9%) and $La(NO_3)_3·6H_2O$ (99.99%) as dopant sources, respectively.

Materials characterization

The morphology and microstructure of samples were observed by field-emission scanning electron microscopy (FESEM; Hitachi, SU8010) and transmission electron microscopy (TEM; JEOL, JEM-1400Plus). Elemental mapping images were obtained from spherical aberration correction electron microscopy (JEOL, JEM-ARM200F). X-ray diffraction (XRD) patterns were collected on a Rigaku Smartlab diffractometer with Cu-Kα radiation (λ = 1.5406 Å). X-ray photoelectron spectroscopy (XPS) measurements were conducted on a Thermo Fisher Scientific K-Alpha instrument. The metal contents of samples were determined by inductively coupled plasma mass spectrometry (ICP-MS; iCAP RQ).

Electrochemical measurements

The electrochemical measurements were performed on a CHI 760E workstation by using the three-electrode system, where the self-supporting MOFs were directly used as the working electrode, saturated Ag/AgCl electrode and graphite rod were used as the reference and counter electrodes, respectively. The Pt/C (20% Pt) and IrO_2 benchmarks on NF were also used for comparison. Firstly, 5 mg of commercial catalysts were dispersed in a mixed solvent of 490 μL of deionized water, 490 μL of absolute ethanol and 20 μL of Nafion by ultrasonication. Then, 50 μL of the ink was dropped onto NF with the loading area of 0.5 cm^2. Linear sweep voltammetry (LSV) measurements were conducted at a scan rate of 5 mV s^{-1} with 95% iR compensation. Electrochemical impedance spectroscopy (EIS) measurements were carried out in the frequency range of 0.1–10^5 Hz with an amplitude of 5 mV. Cyclic voltammetry (CV) measurements were performed at different scan rates (50, 100, 150 and 200 mV s^{-1}) to evaluate the double-layer capacitance (C_{dl}). Electrochemically active surface area (ECSA) was calculated by the following equation: ECSA = C_{dl}/C_s, C_s = 0.06 mF cm^{-2}. The measured potentials were calibrated to reversible hydrogen electrode (RHE) according to the equation: $E_{RHE} = E_{Ag/AgCl} + 0.197\ V + 0.059 \times pH$.

Computational details

All density functional theory (DFT) calculations were conducted in the Vienna ab initio simulation package (VASP) code[1-3]. The ionic cores were described by the projector-augmented wave (PAW) pseudo-potential[4, 5]. The cut-off energy for plane wave expansion was set to 400 eV. The electronic self-consistent-loop criterion was set to 10^{-8} eV. During geometry optimization, the structures were relaxed to forces on all atoms smaller than 0.02 eV/Å. Gaussian smearing method was used with 0.05 eV width. To avoid the interaction among slabs, the vacuum spacing between periodically repeated slabs was set to 15 Å. The Brillouin zone integration was carried out with the 4×8×1 Monkhorst-Pack k-point sampling for all structures. DFT + U method was applied to better describe the systems. U = 4.3 and 0, U = 3.8 and 0, as well as U = 5.5 and 0.5 were chosen for Fe, Ni and Ce in OER and HER calculations, respectively.

During optimization of H*, OH*, O* and OOH* adsorption, the substrate atoms were fixed to allow a time-efficient relaxation of the adsorbed species. The adsorption energies (E_{ads}) can be obtained by the equation: $E_{ads} = E_{ad/sub} - E_{ad} - E_{sub}$
where $E_{ad/sub}$, E_{ad} and E_{sub} are the total energies of the optimized adsorbate/substrate system, the adsorbate in the structure and the clean substrate, respectively.

Gibbs free energy was calculated as follow: $\Delta G = \Delta E_{DFT} + \Delta ZPE - T\Delta S - eU$
where ΔE_{DFT} is the calculated reaction energy by DFT method, ΔZPE is the change of zero-point energy and ΔS is the change of entropy.

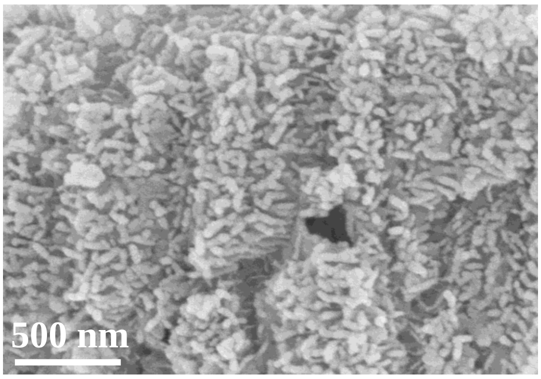

Fig. S1 SEM image of NiFe-MOF.

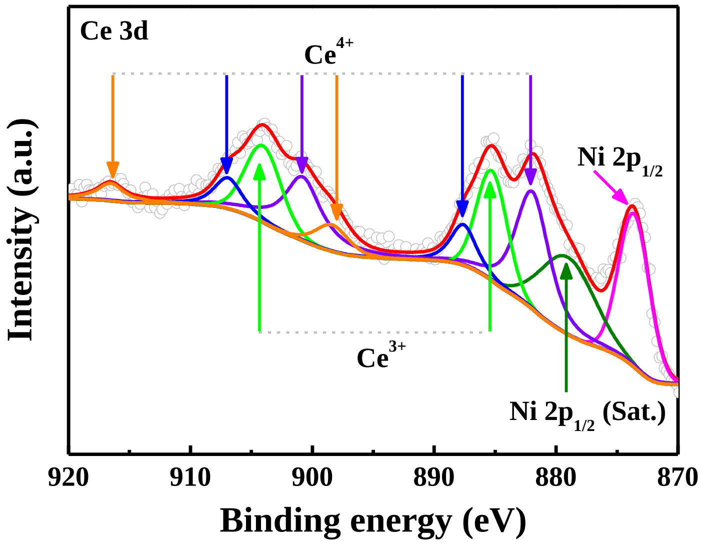

Fig. S2 High-resolution Ce 3d spectrum of CeNiFe-MOF.

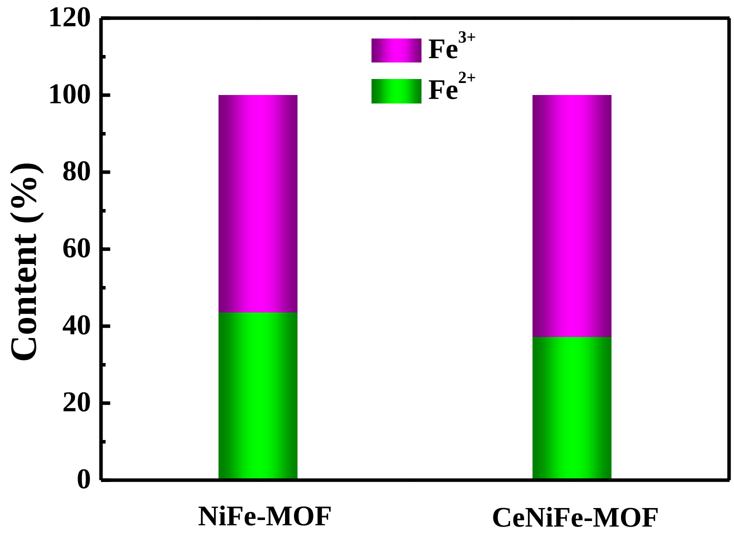

Fig. S3 The content of Fe^{2+} and Fe^{3+} obtained from XPS analysis.

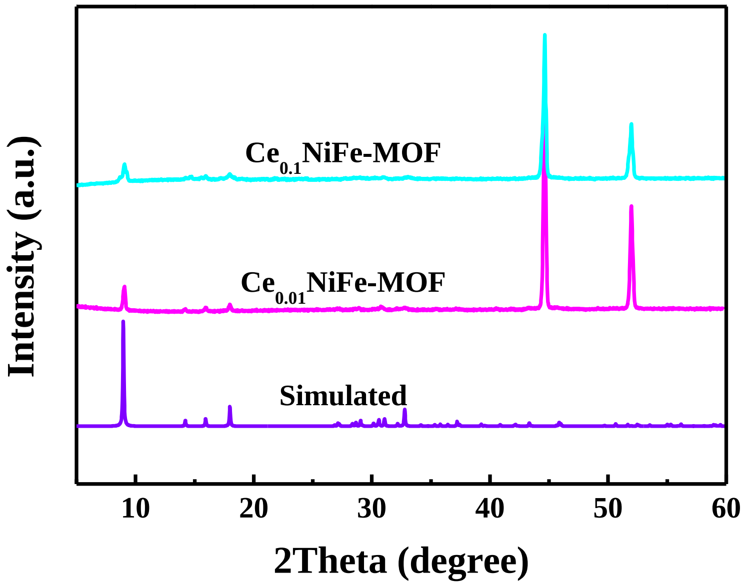

Fig. S4 XRD patterns of $Ce_{0.01}$NiFe-MOF and $Ce_{0.1}$NiFe-MOF.

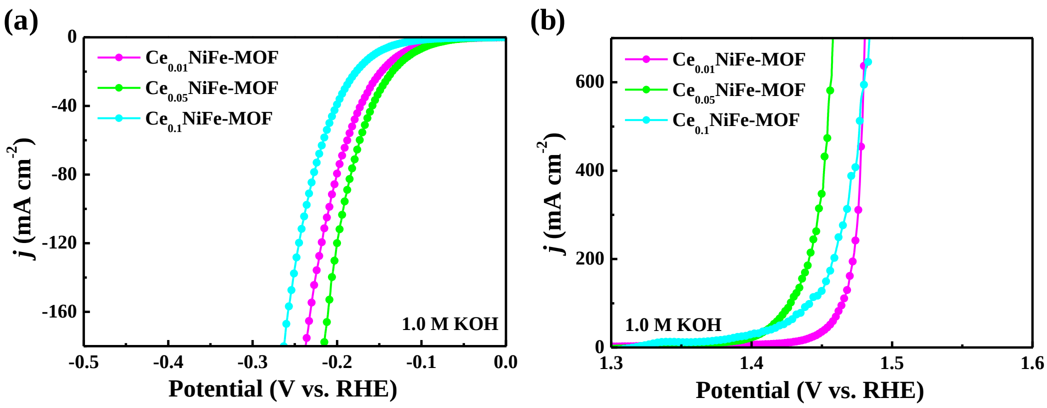

Fig. S5 (a) HER and (b) OER polarization curves of Ce_xNiFe-MOF in 1.0 M KOH.

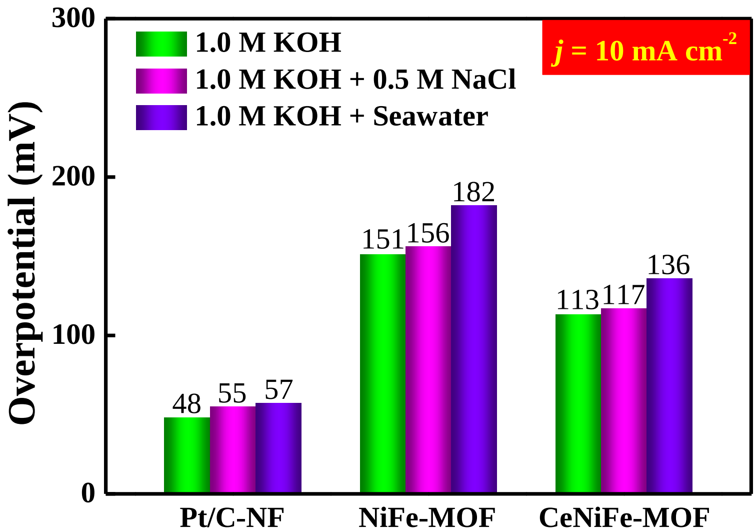

Fig. S6 Overpotential comparison of CeNiFe-MOF, NiFe-MOF and commercial Pt/C in different electrolytes.

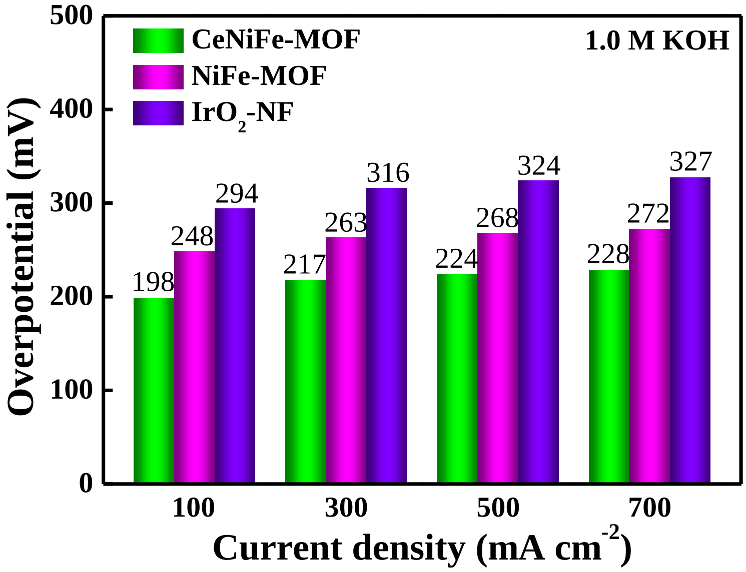

Fig. S7 Overpotential comparison of CeNiFe-MOF, NiFe-MOF and commercial IrO_2 at different current densities in 1.0 M KOH.

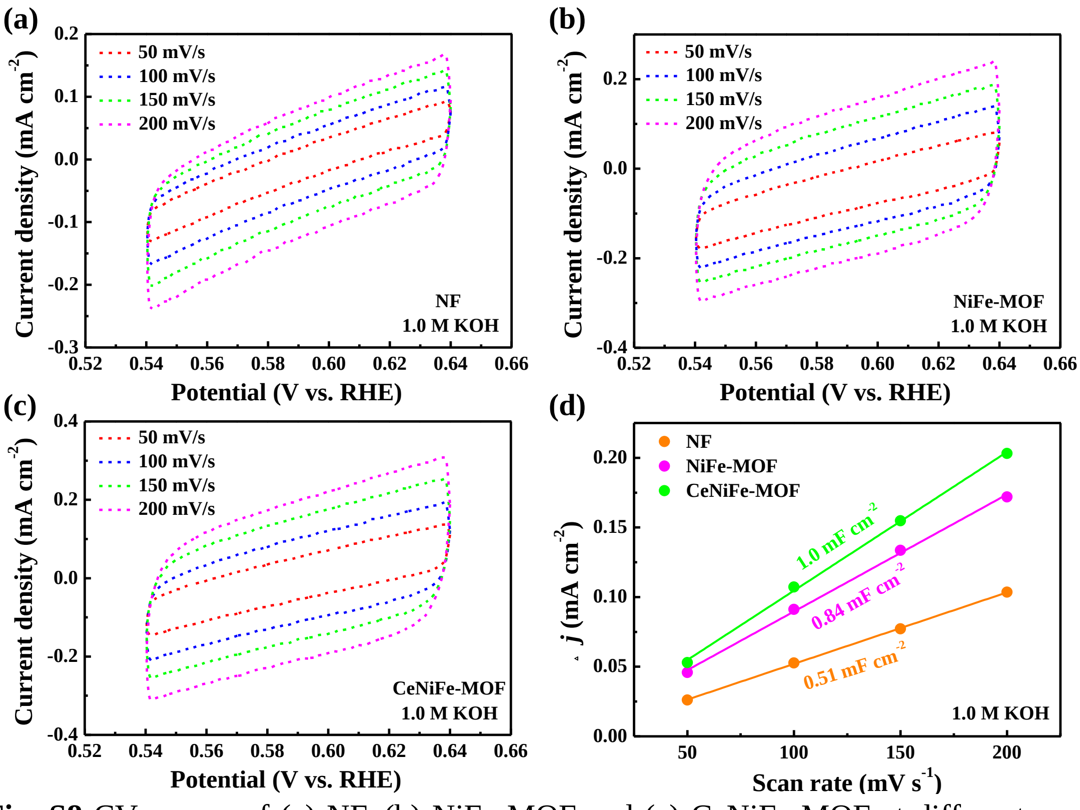

Fig. S8 CV curves of (a) NF, (b) NiFe-MOF and (c) CeNiFe-MOF at different scan rates in 1.0 M KOH. (d) The corresponding double-layer capacitance.

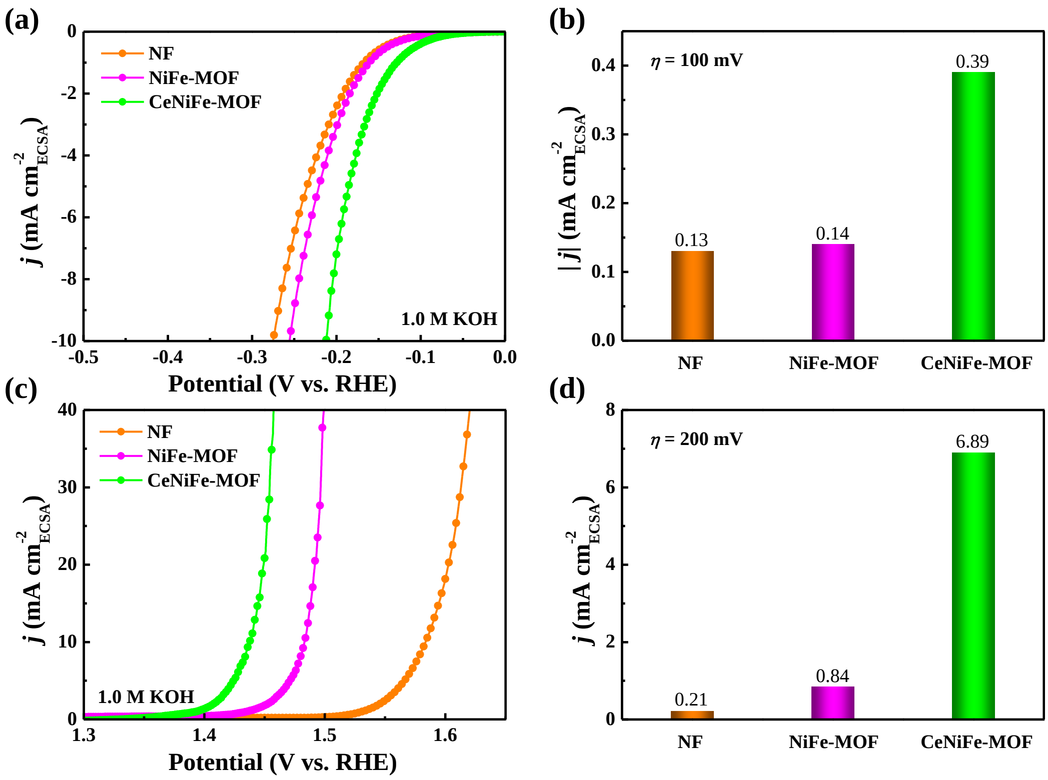

Fig. S9 (a) The ECSA-normalized HER polarization curves in 1.0 M KOH. (b) The corresponding specific activities at an overpotential of 100 mV. (c) The ECSA-normalized OER polarization curves in 1.0 M KOH. (d) The corresponding specific activities at 1.43 V vs. RHE.

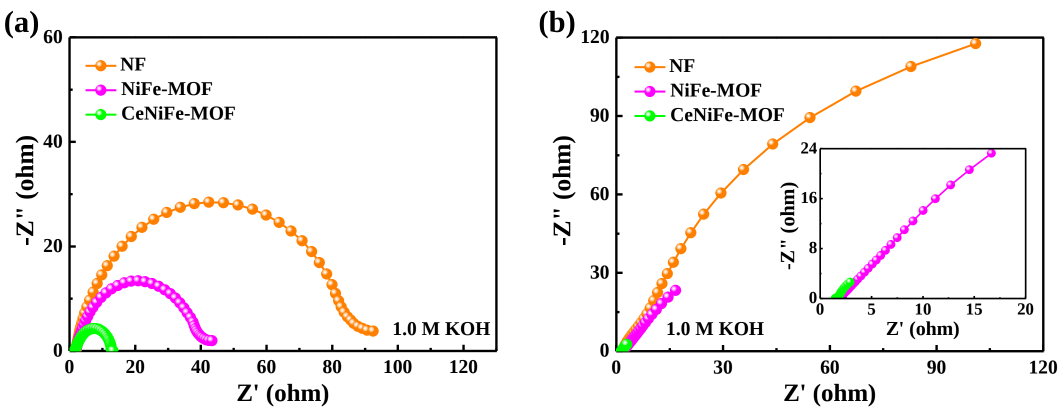

Fig. S10 Nyquist plots measured at the overpotential of (a) 150 mV for HER and (b) 200 mV for OER in 1.0 M KOH.

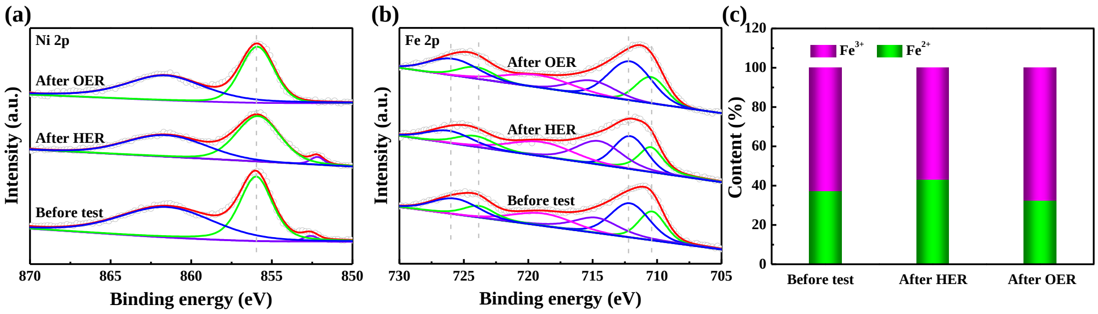

Fig. S11 (a) Ni 2p and (b) Fe 2p spectra of CeNiFe-MOF after water electrolysis test in 1.0 M KOH. (c) The content of Fe^{2+} and Fe^{3+} obtained from XPS analysis.

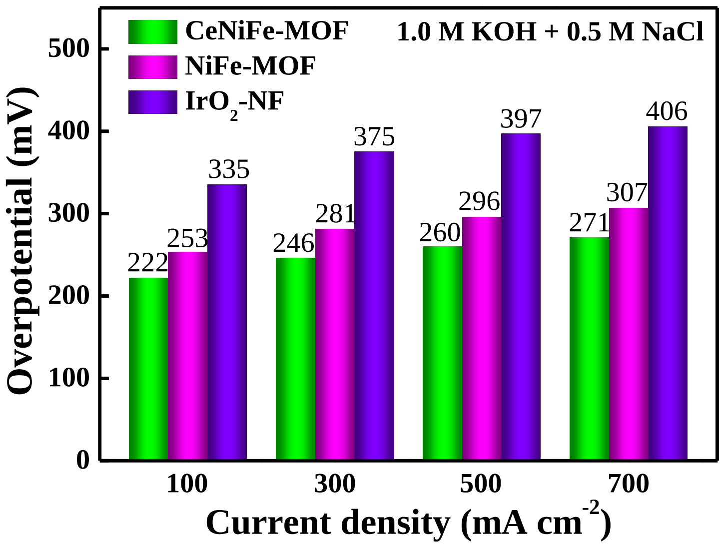

Fig. S12 Overpotential comparison of CeNiFe-MOF, NiFe-MOF and commercial IrO_2 at different current densities in 1.0 M KOH + 0.5 M NaCl.

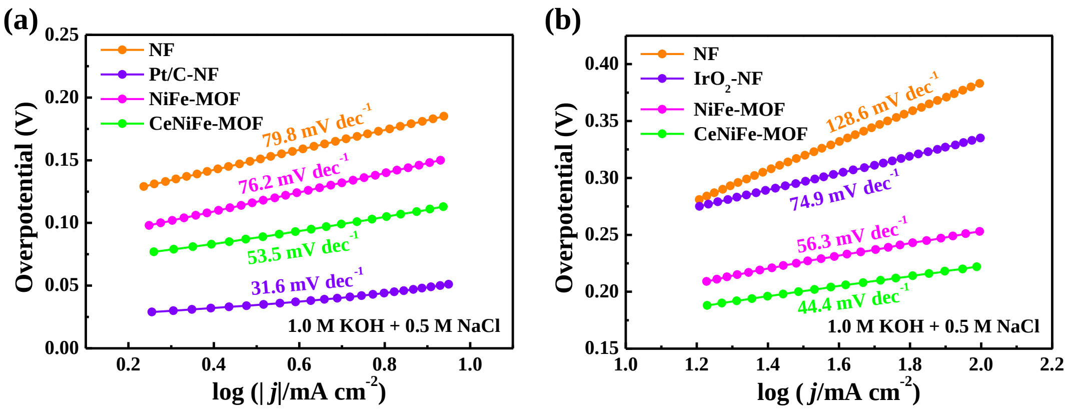

Fig. S13 Tafel slopes for (a) HER and (b) OER in 1.0 M KOH + 0.5 M NaCl.

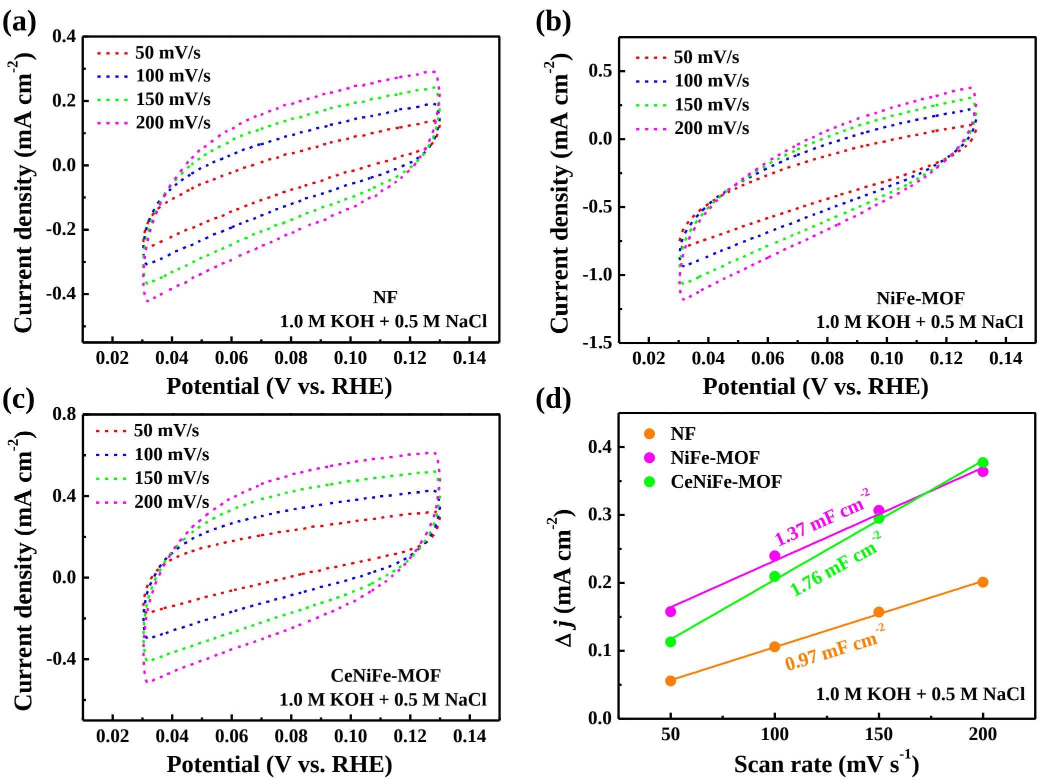

Fig. S14 CV curves of (a) NF, (b) NiFe-MOF and (c) CeNiFe-MOF at different scan rates in 1.0 M KOH + 0.5 M NaCl. (d) The corresponding double-layer capacitance.

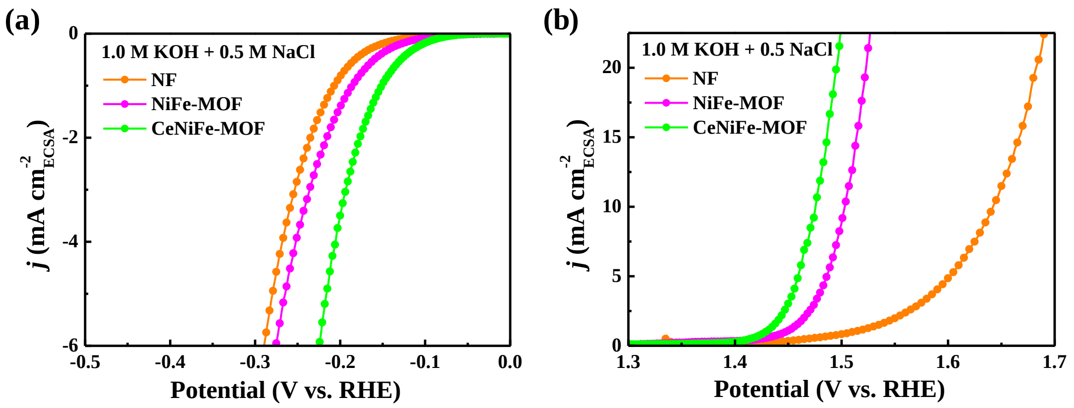

Fig. S15 The ECSA-normalized (a) HER and (b) OER polarization curves in 1.0 M KOH + 0.5 M NaCl.

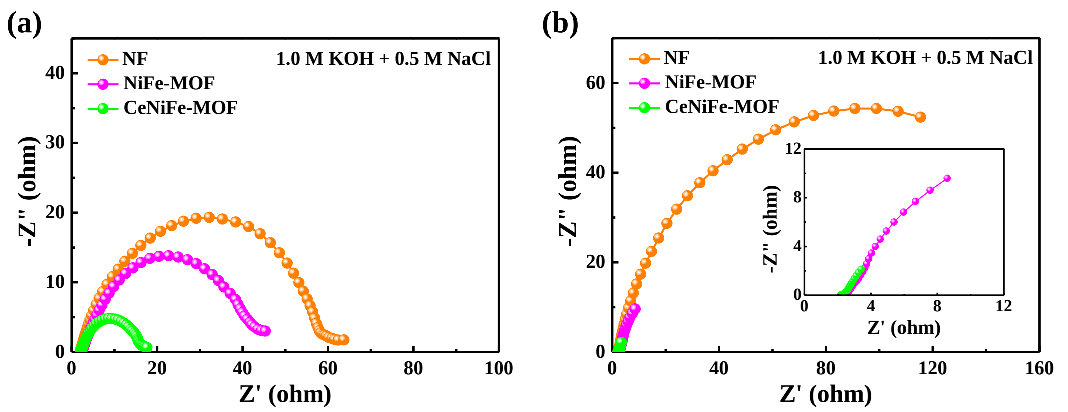

Fig. S16 Nyquist plots measured at the overpotential of (a) 150 mV for HER and (b) 200 mV for OER in 1.0 M KOH + 0.5 M NaCl.

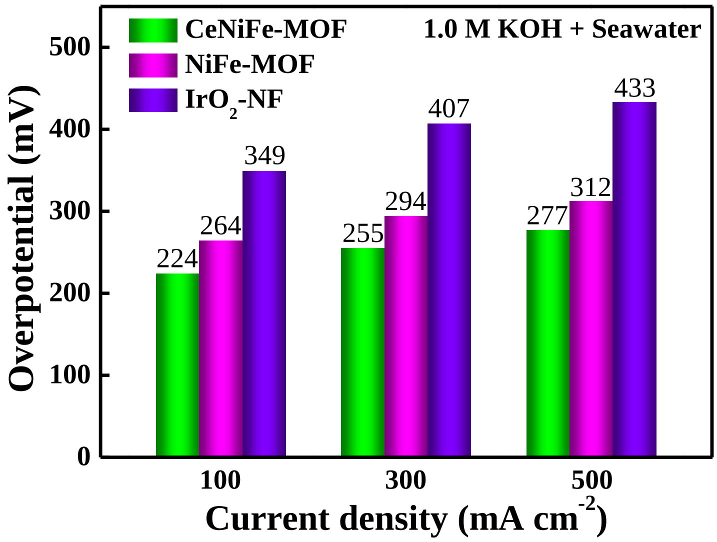

Fig. S17 Overpotential comparison of CeNiFe-MOF, NiFe-MOF and commercial IrO_2 at different current densities in 1.0 M KOH + seawater.

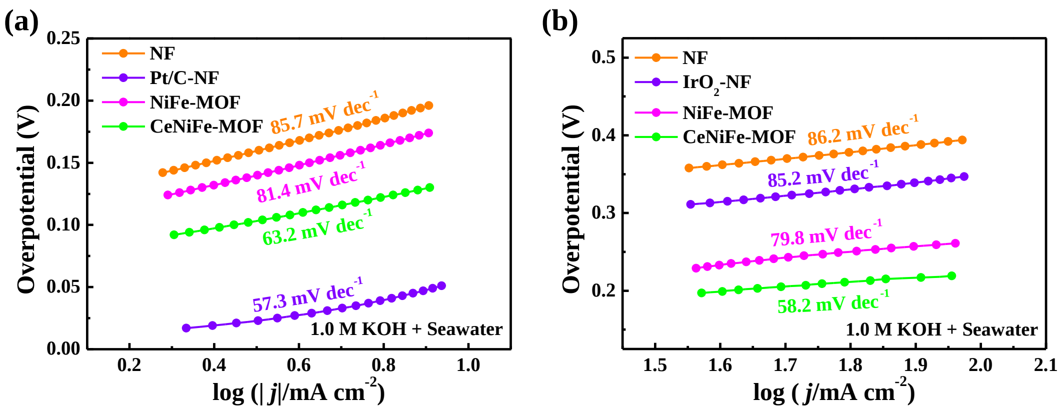

Fig. S18 Tafel slopes for (a) HER and (b) OER in 1.0 M KOH + seawater.

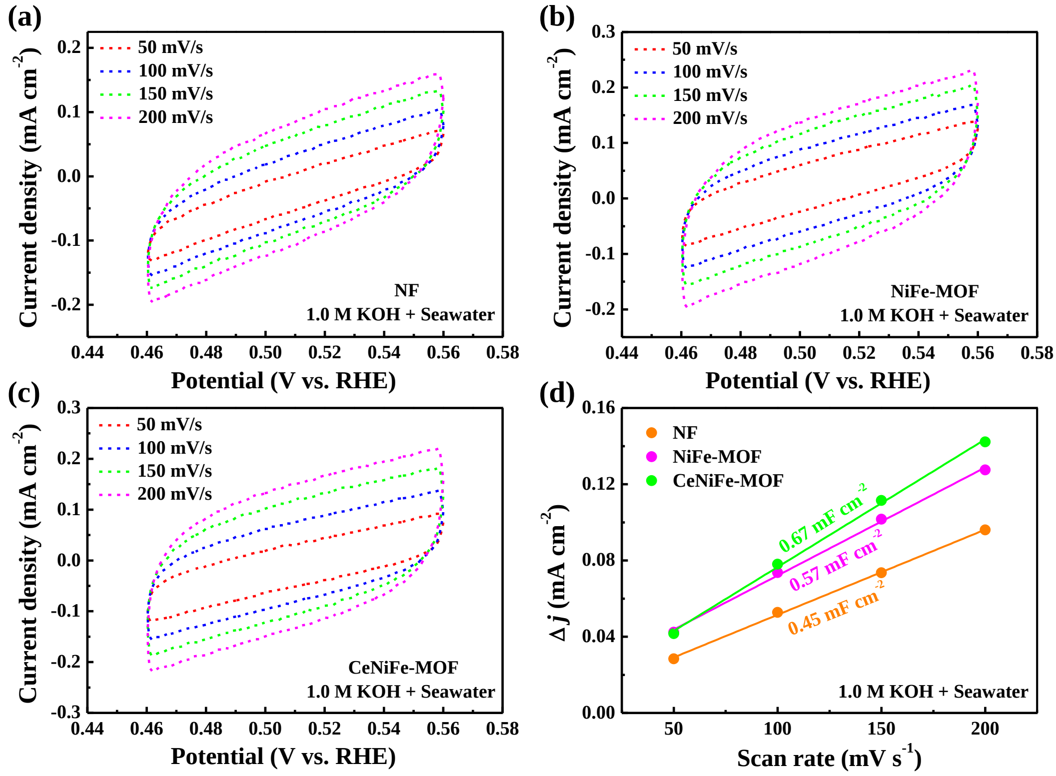

Fig. S19 CV curves of (a) NF, (b) NiFe-MOF and (c) CeNiFe-MOF at different scan rates in 1.0 M KOH + seawater. (d) The corresponding double-layer capacitance.

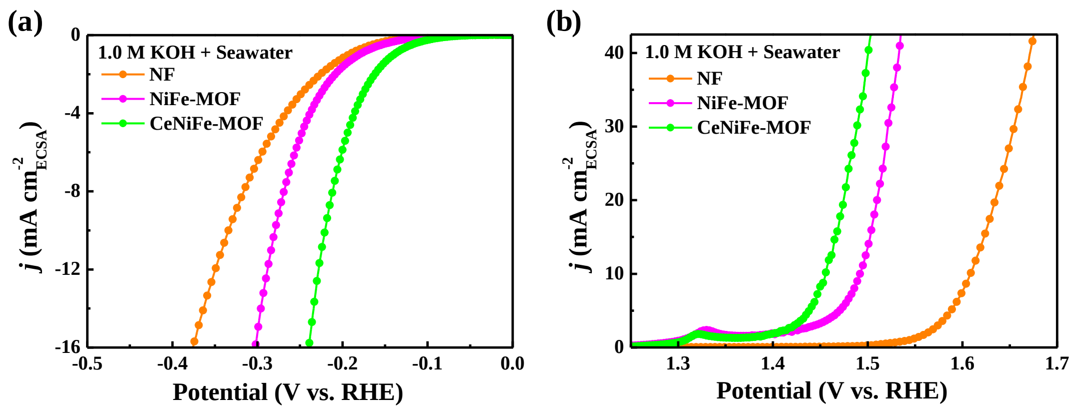

Fig. S20 The ECSA-normalized (a) HER and (b) OER polarization curves in 1.0 M KOH + seawater.

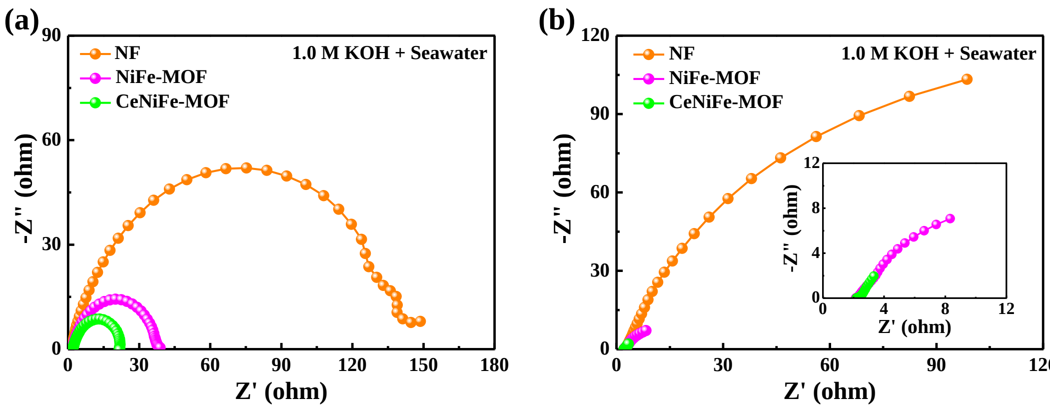

Fig. S21 Nyquist plots measured at the overpotential of (a) 150 mV for HER and (b) 200 mV for OER in 1.0 M KOH + seawater.

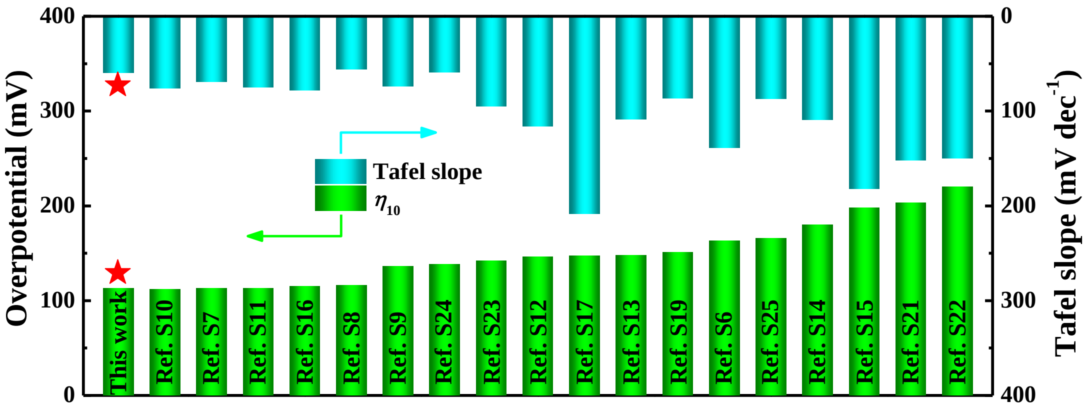

Fig. S22 Comparison of HER performance of as-prepared CeNiFe-MOF with other MOF-based electrocatalysts in 1.0 M KOH.

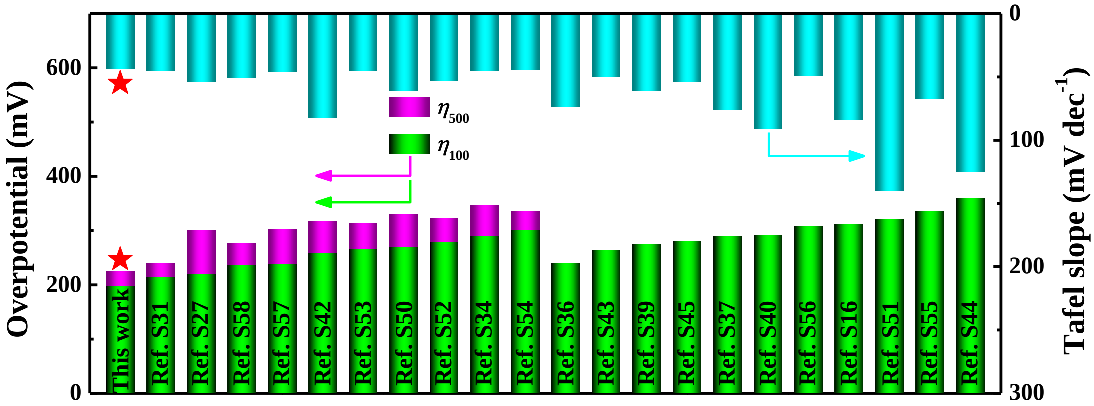

Fig. S23 Comparison of OER performance of as-prepared CeNiFe-MOF with other MOF-based electrocatalysts in 1.0 M KOH.

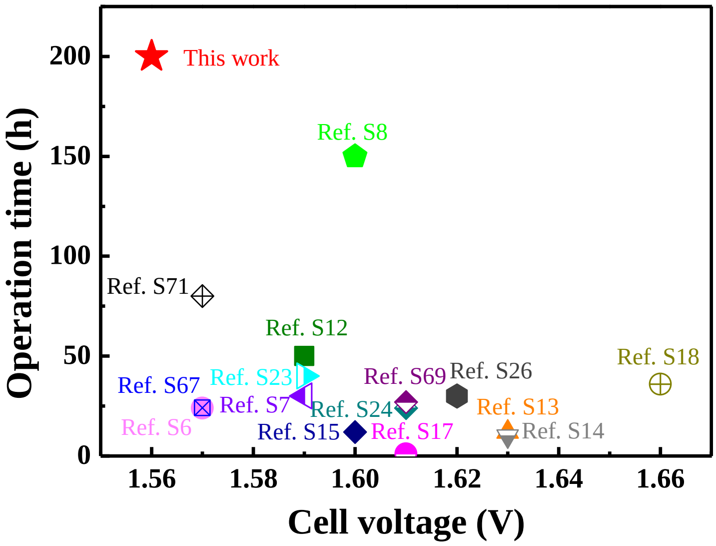

Fig. S24 Comparison of alkaline freshwater splitting performance of as-prepared CeNiFe-MOF with other MOF-based electrocatalysts.

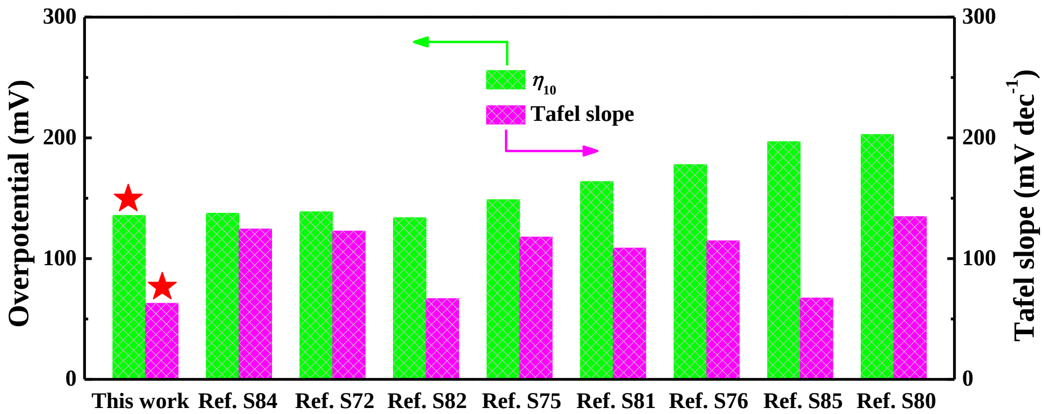

Fig. S25 Comparison of HER performance of as-prepared CeNiFe-MOF with other advanced electrocatalysts in 1.0 M KOH + seawater.

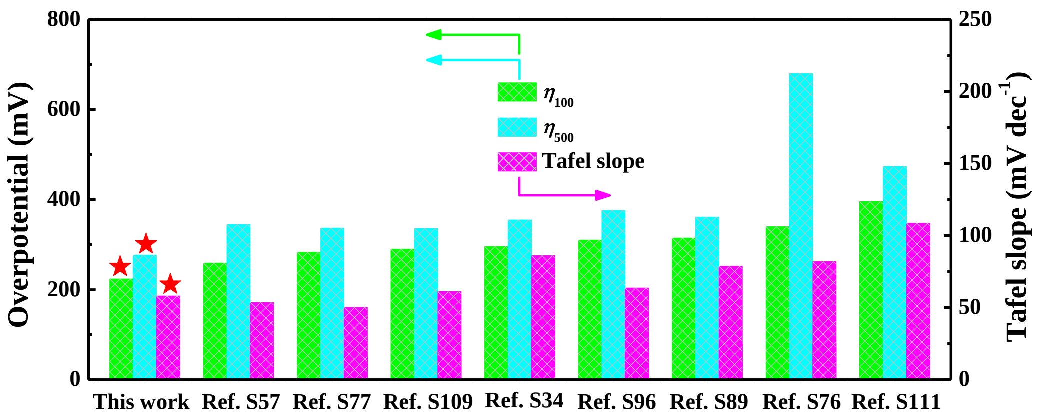

Fig. S26 Comparison of OER performance of as-prepared CeNiFe-MOF with other advanced electrocatalysts in 1.0 M KOH + seawater.

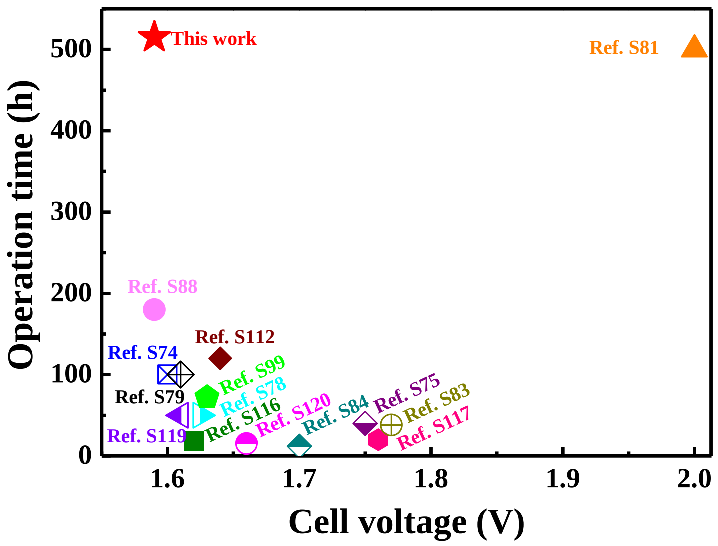

Fig. S27 Comparison of alkaline seawater splitting performance of as-prepared CeNiFe-MOF with other advanced electrocatalysts.

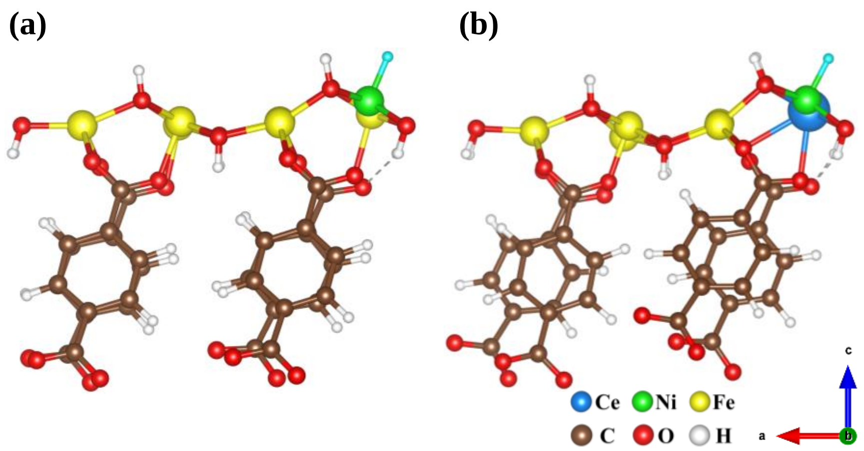

Fig. S28 The optimized structures of adsorbed H* on (a) NiFe-MOF/Ni and (b) CeNiFe-MOF/Ni.

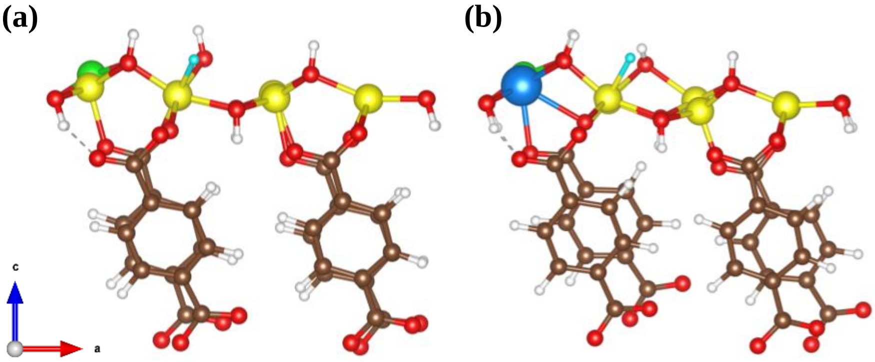

Fig. S29 The optimized structures of adsorbed H* on (a) NiFe-MOF/Fe and (b) CeNiFe-MOF/Fe.

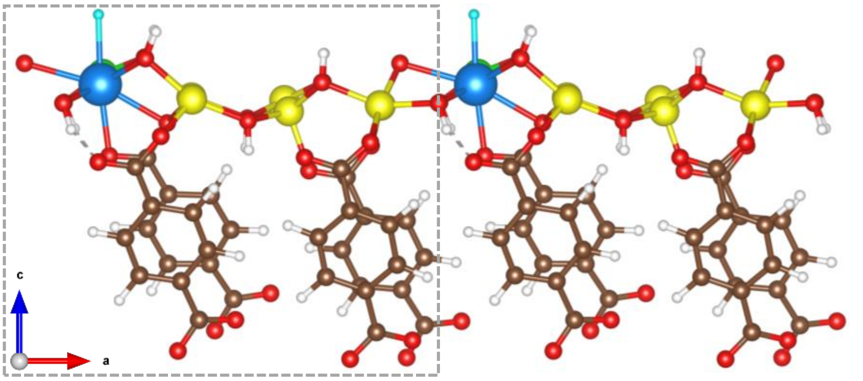

Fig. S30 The optimized structures of adsorbed H* on CeNiFe-MOF/Ce.

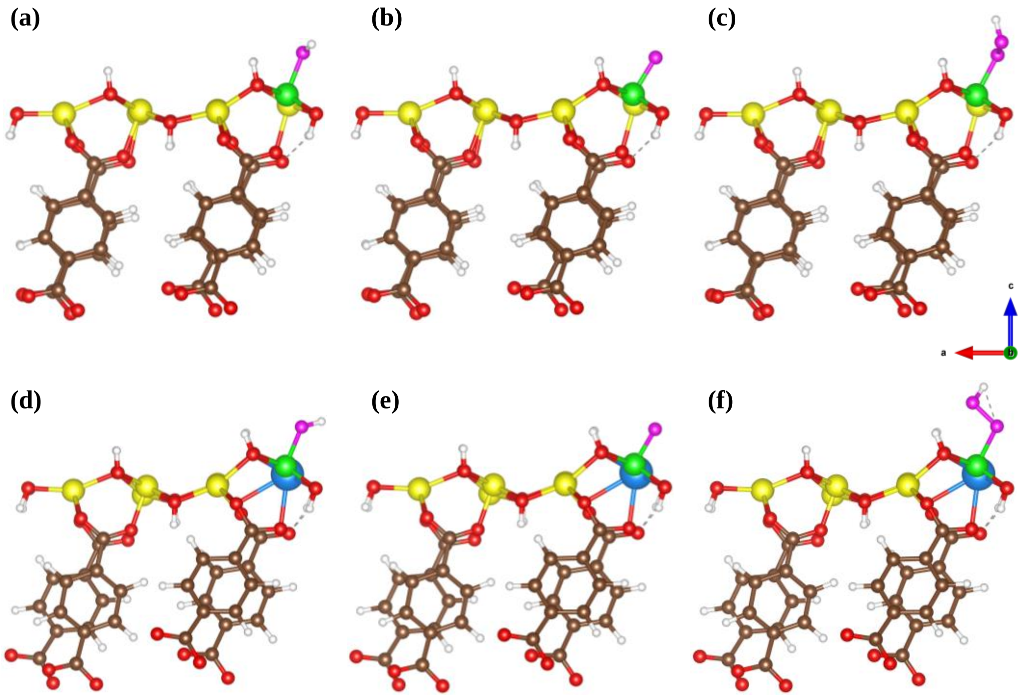

Fig. S31 The optimized structures of adsorbed intermediates on (a–c) NiFe-MOF/Ni and (d–f) CeNiFe-MOF/Ni.

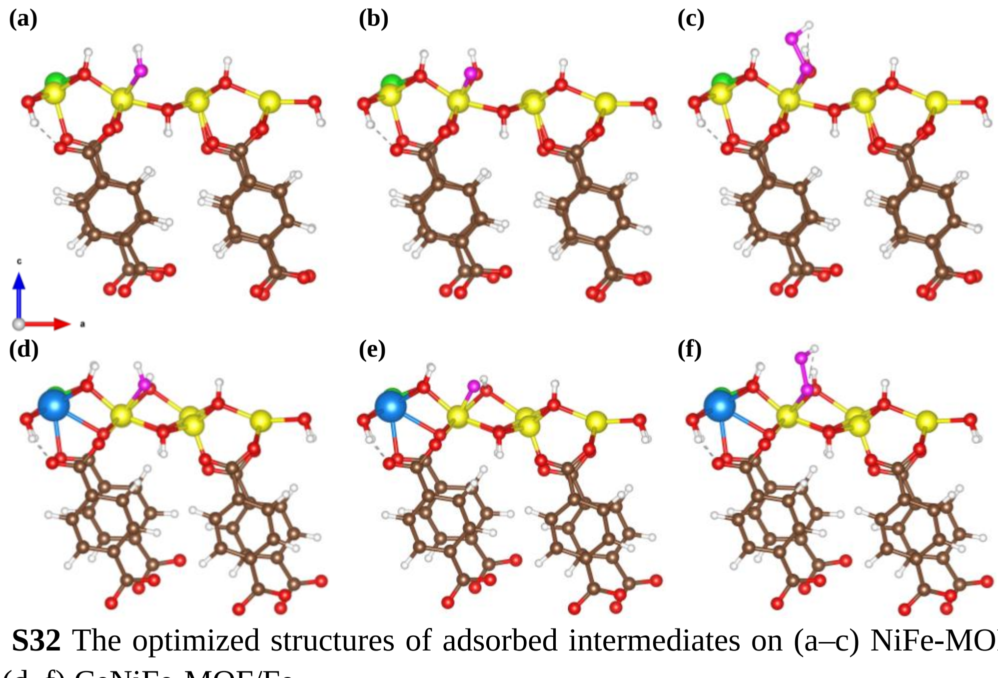

Fig. S32 The optimized structures of adsorbed intermediates on (a–c) NiFe-MOF/Fe and (d–f) CeNiFe-MOF/Fe.

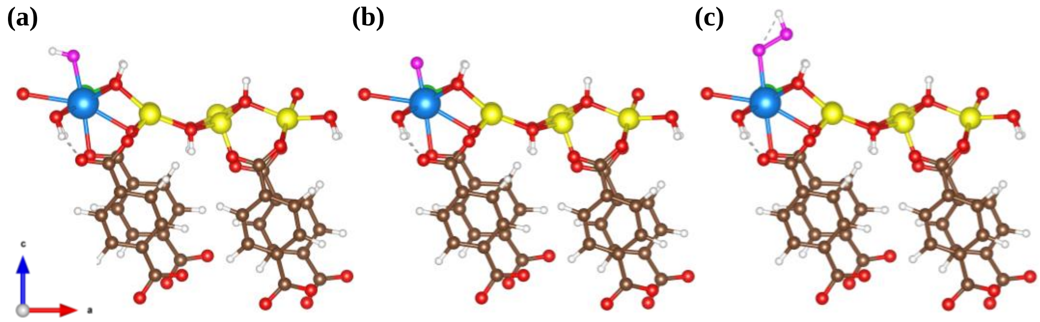

Fig. S33 The optimized structures of adsorbed intermediates on CeNiFe-MOF/Ce.

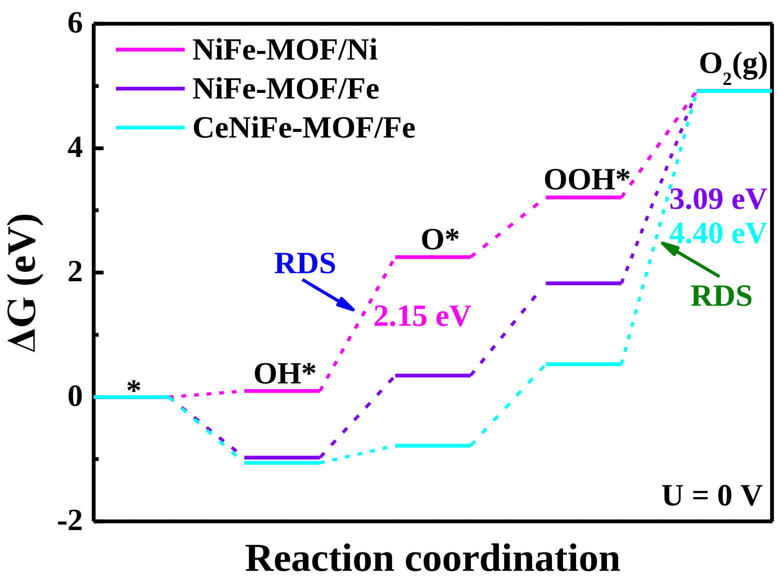

Fig. S34 The free energy diagram for OER process on NiFe-MOF/Ni, NiFe-MOF/Fe and CeNiFe-MOF/Fe.

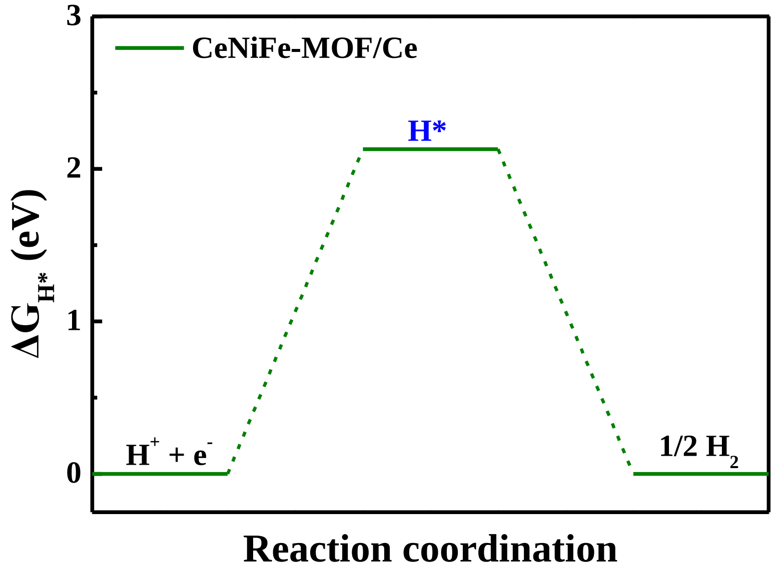

Fig. S35 The free energy diagram for HER process on CeNiFe-MOF/Ce.

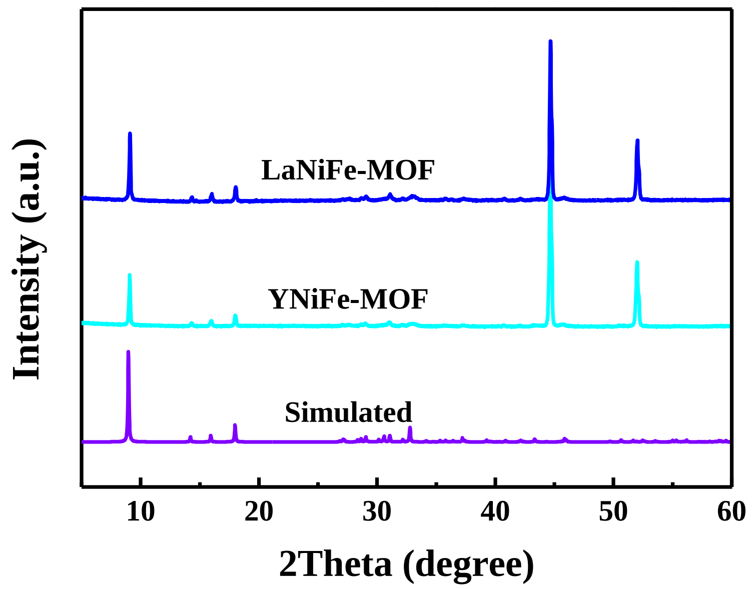

Fig. S36 XRD patterns of YNiFe-MOF and LaNiFe-MOF.

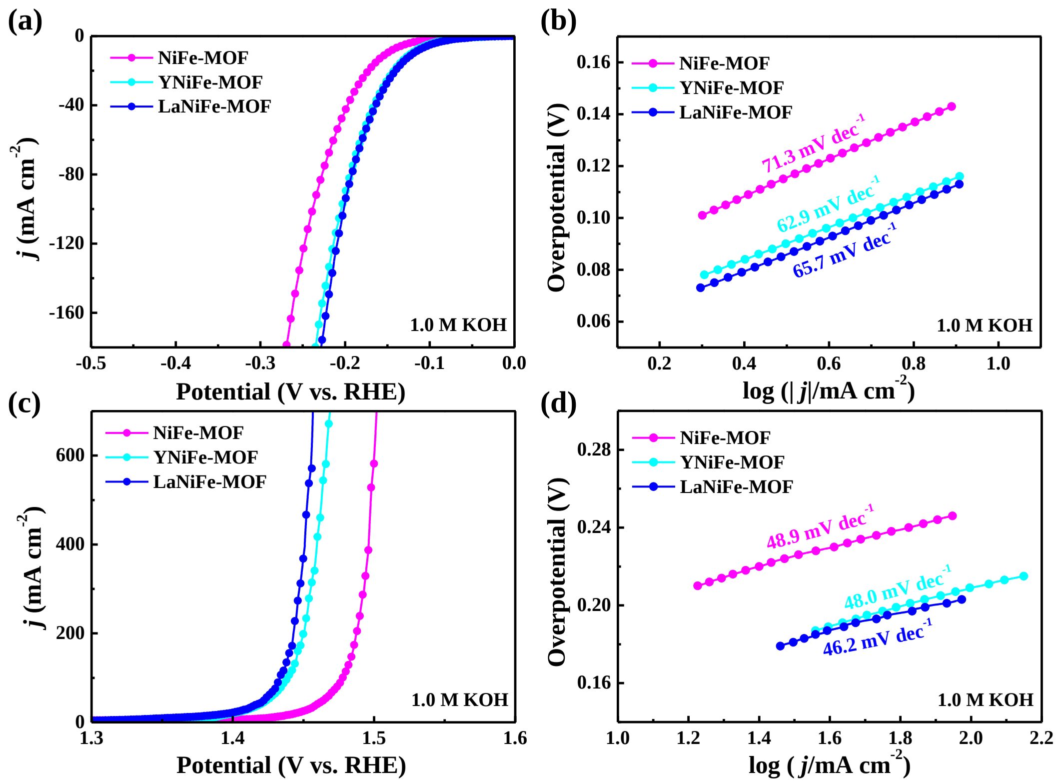

Fig. S37 Electrochemical performance of the samples in 1.0 M KOH. (a) HER polarization curves and (b) the corresponding Tafel slopes. (c) OER polarization curves and (d) the corresponding Tafel slopes.

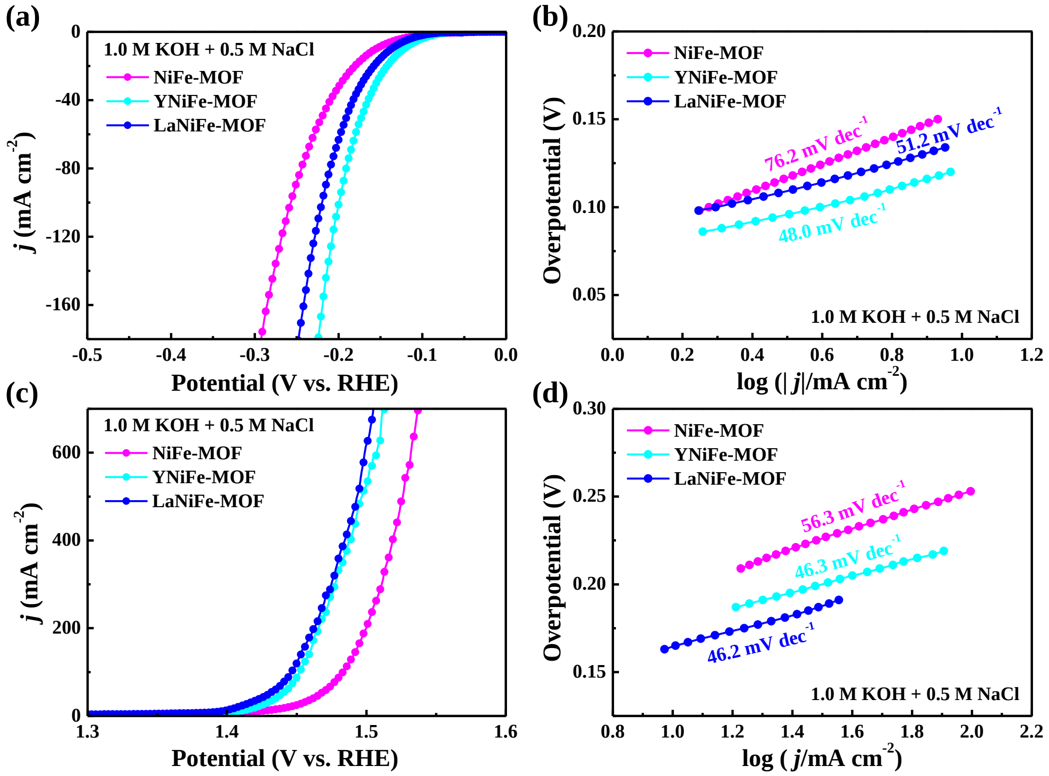

Fig. S38 Electrochemical performance of the samples in 1.0 M KOH + 0.5 M NaCl. (a) HER polarization curves and (b) the corresponding Tafel slopes. (c) OER polarization curves and (d) the corresponding Tafel slopes.

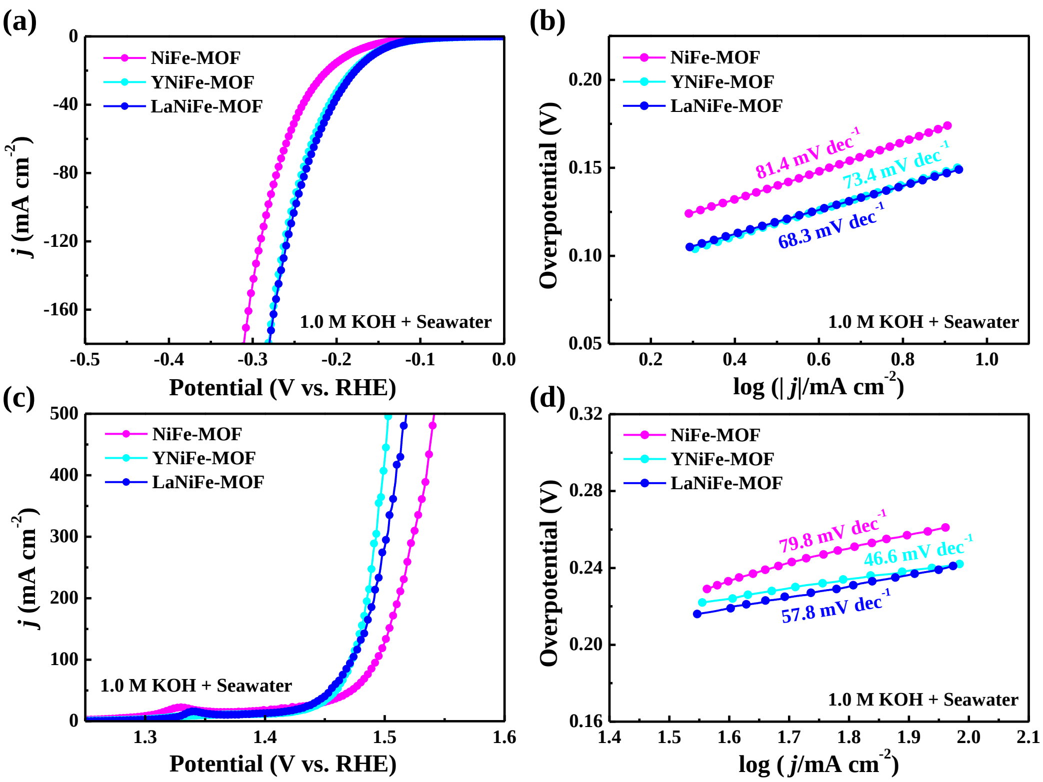

Fig. S39 Electrochemical performance of the samples in 1.0 M KOH + seawater. (a) HER polarization curves and (b) the corresponding Tafel slopes. (c) OER polarization curves and (d) the corresponding Tafel slopes.

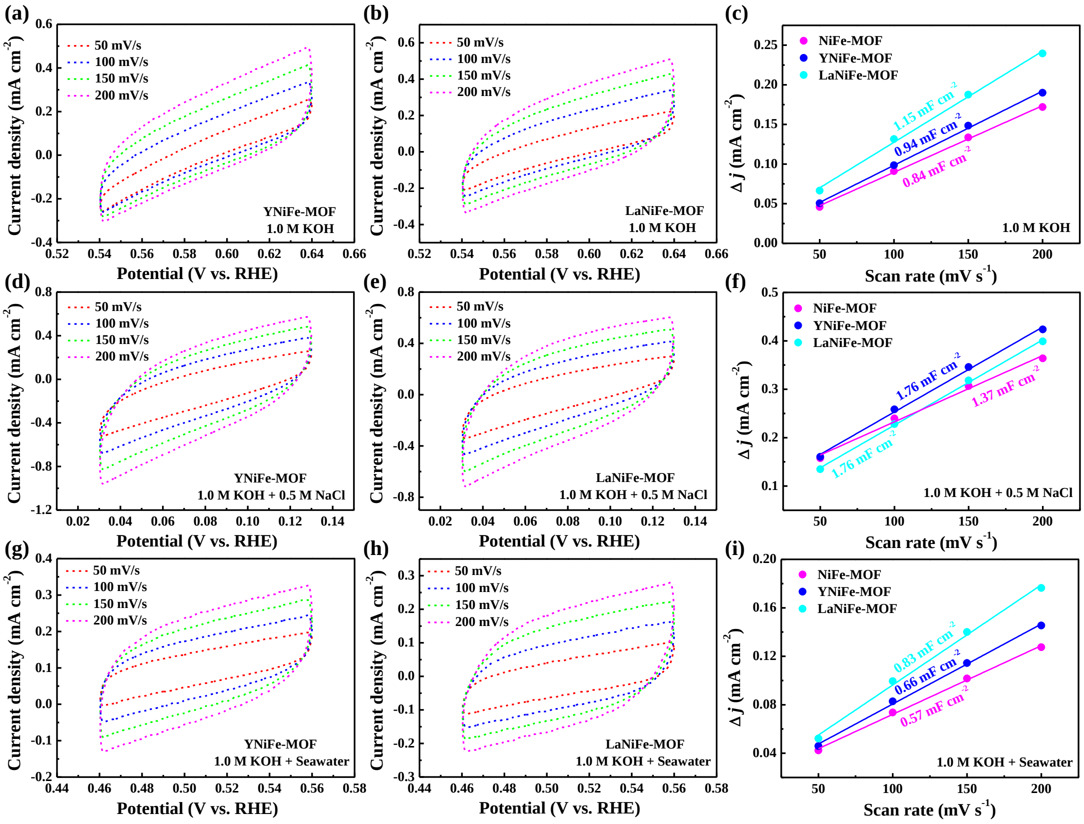

Fig. S40 CV curves of YNiFe-MOF and LaNiFe-MOF in (a, b) 1.0 M KOH, (d, e) 1.0 M KOH + 0.5 M NaCl and (g, h) 1.0 M KOH + seawater. (c, f, i) The corresponding double-layer capacitance.

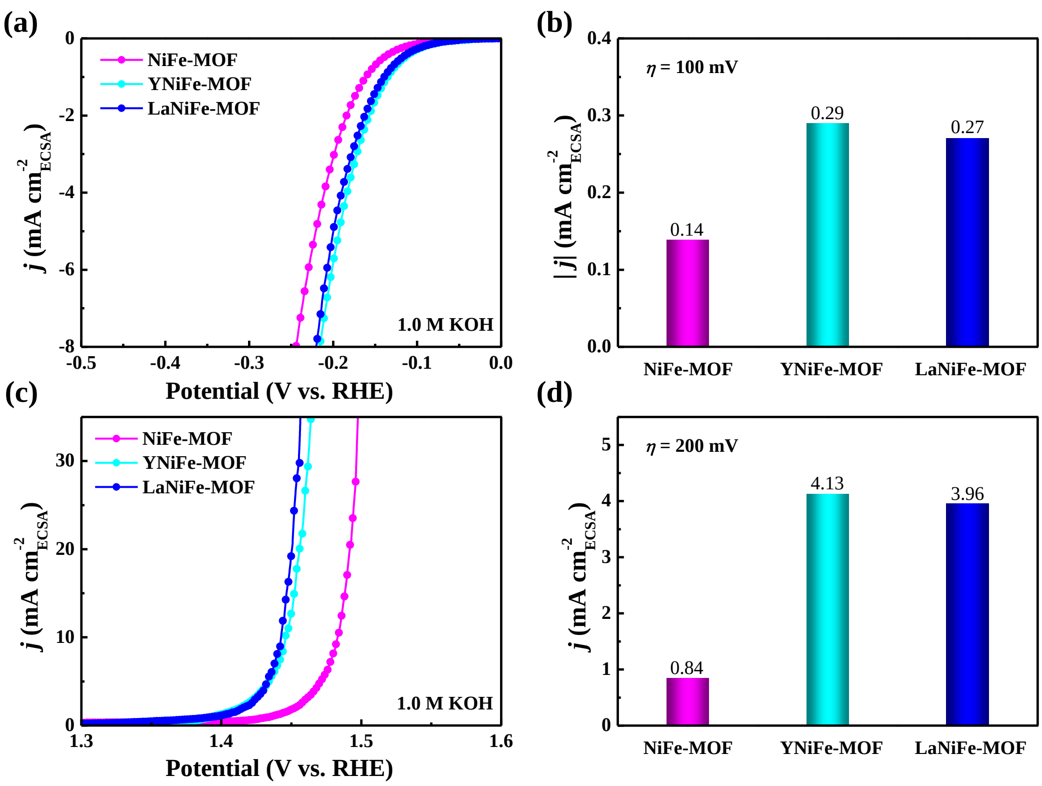

Fig. S41 (a) The ECSA-normalized HER polarization curves in 1.0 M KOH. (b) The corresponding specific activities at an overpotential of 100 mV. (c) The ECSA-normalized OER polarization curves in 1.0 M KOH. (d) The corresponding specific activities at 1.43 V vs. RHE.

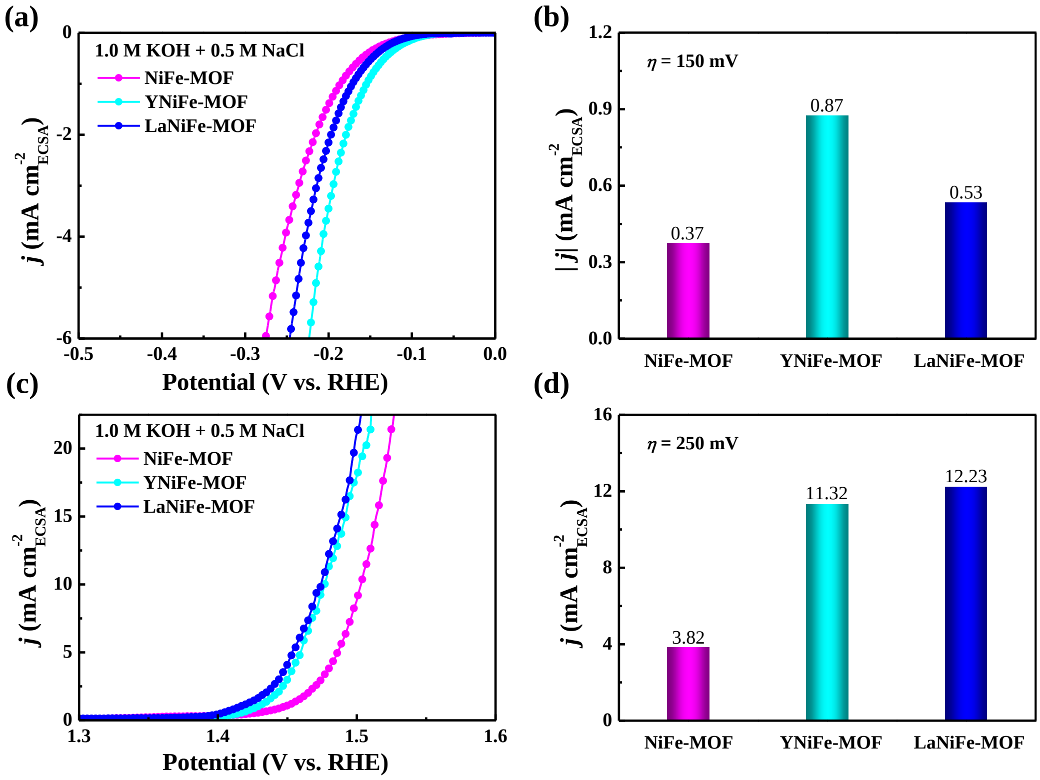

Fig. S42 (a) The ECSA-normalized HER polarization curves in 1.0 M KOH + 0.5 M NaCl. (b) The corresponding specific activities at an overpotential of 150 mV. (c) The ECSA-normalized OER polarization curves in 1.0 M KOH + 0.5 M NaCl. (d) The corresponding specific activities at 1.48 V vs. RHE.

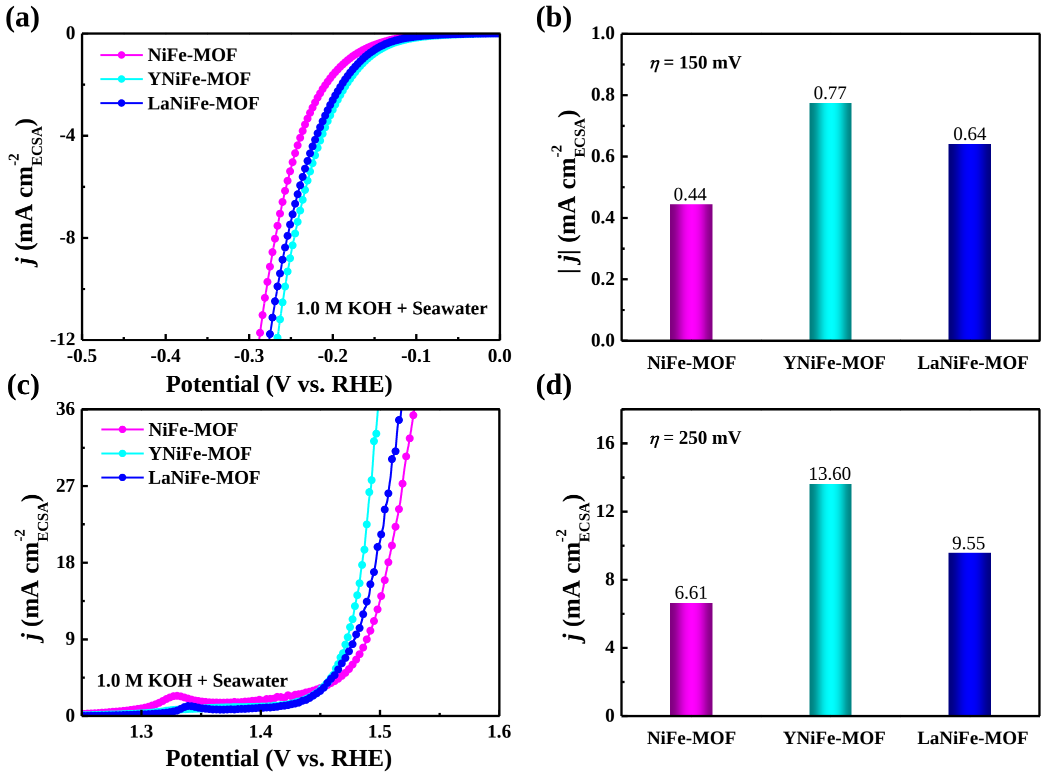

Fig. S43 (a) The ECSA-normalized HER polarization curves in 1.0 M KOH + seawater. (b) The corresponding specific activities at an overpotential of 150 mV. (c) The ECSA-normalized OER polarization curves in 1.0 M KOH + seawater. (d) The corresponding specific activities at 1.48 V vs. RHE.

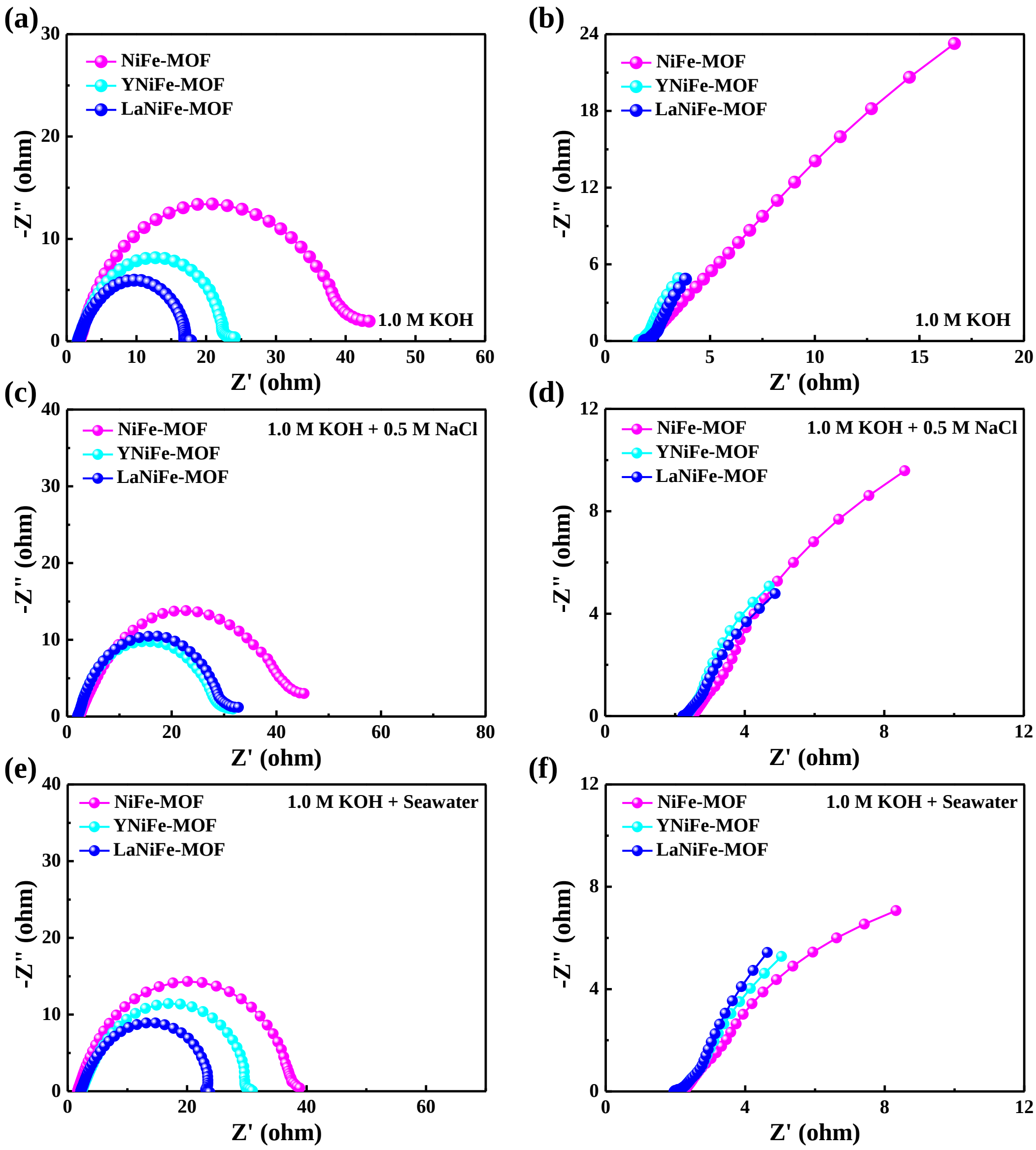

Fig. S44 Nyquist plots for (a, c, e) HER and (b, d, f) OER measured in different electrolytes.

Table S1. Comparison of HER activity of MOF-based electrocatalysts in 1.0 M KOH.

Electrocatalysts	Substrate	η_{10} (mV)	Tafel slope (mV dec^{-1})	Ref.
CeNiFe-MOF		113	59.4	This
YNiFe-MOF	NF	122	62.9	work
LaNiFe-MOF		119	65.7	
NiFe-MOF-5	NF	163	139	6
NiFe(dobpdc)	NF	113	69	7
Fe-Co-Ni MOF	NF	116	56	8
NiYCe-MOF/NF	NF	136	74	9
$Fe(OH)_x$@Cu-MOF	CP	112	76	10
S-NiBDC	NF	113	75	11
LIA-Ni-BDC	NF	146	116	12
CdFe-BDC	NF	148	108.71	13
BP@MOF	GCE	180	109	14
Fe_2V-MOF	NF	198	182	15
Co-MOF/NF	NF	115	78	16
VFe-MOF@NF	NF	147	208.25	17
CoFe-MOF@Pa	NF	255	/	18
Fe@Co-MOF-3	NF	151	86.54	19
Co/Cu-MOF(3)	GCE	391	94	20
CoNi-MOFs-DBD	NF	203	152.2	21
MXene@Ce-MOF	/	220	149.9	22
NiFe-MOF/$NiSe_x$/NF	NF	142	94.7	23
Ni@CoO@Co-MOFC	NF	138	59	24
CuO@NH_2-UiO-66/NF	NF	166	87	25
FeCoMnNi-MOF-74/NF	NF	108	72.89	26

NF: nickel foam; CP: carbon paper; GCE: glassy carbon electrode

Table S2. Comparison of OER activity of MOF-based electrocatalysts in 1.0 M KOH.

Electrocatalysts	Substrate	η_{100} (mV)	η_{500} (mV)	Tafel slope (mV dec^{-1})	Ref.
CeNiFe-MOF		198	224	43.5	This
YNiFe-MOF	NF	209	233	48.0	work
LaNiFe-MOF		203	223	46.2	
CdFe-BDC	NF	290	/	44.57	13
Co-MOF/NF	NF	311	/	84	16
6%LS-CMMOFs/NF	NF	220	300	54	27
Fe-NiHF	GCE	340	/	44	28
Ni-BDC/NM88B(Fe)	NF	232	/	37.6	29
NiFc-MOF/NF	NF	241	/	44.1	30
NiFc'Fc/NF	NF	213	240	45	31
NiFe-MOF	CFC	/	297	49.1	32
NiFe-MOF/G	GCE	326	/	49	33
NiFe-MOF@NiS/NF	NF	290	346	45.1	34
NiFe MOF/NF	NF	256	/	40	35
NiFe-MOF/FF	FF	240	/	73.4	36
NiV-MOF NAs	NF	290	/	76.2	37
FeNi-MOFs/NF	NF	266	/	52.4	38
NiFe-LDH/MOF	NF	275	/	61	39
ZnFe-BDC-0.75	NF	292	/	90.72	40
Ir@NiFe-MOF/NF	NF	251	298	38.5	41
$Dy_{0.05}$Fe-MOF/NF	NF	258	318	82	42
FeNi-LDH/MOF/CC	CC	263	/	50	43
FeMOF/NiMOF/NF	NF	359	/	125.3	44
NiFe(DMBD)-MOF/NF	NF	280	/	54.3	45
NiFe-MOF-BF_4^--0.3 NSs	GCE	278	/	41	46
Fe-doped-(Ni-MOFs)/FeOOH	NF	278	/	50	47
Ce-NiBDC/OG	GF	337	/	46	48
Ce-m-$Ni(OH)_2$@Ni-MOF	NF	272	/	43.2	49
Cu-Fe-NH_2 MOF/NF	NF	270	330	60.8	50
Co/Mn@CNDs-MOF	NF	320	/	140	51
Fe-MOF-U	NF	278	322	53.3	52
MIL-53(Fe)-2OH	NF	266	314	45.4	53
$_{AOG}$TM-PG[R]	NF	300	335	44.3	54
CoNiRu-NT	NF	335	/	67	55
Ni NDC-Co/CP	CP	308	/	49.1	56
HMIL-88@PPy-TA	NF	238	303	45.8	57
CoNi-LDH/Fe MOF/NF	NF	235	277	50.7	58
MIL-(IrNiFe)@NF	NF	230(η_{50})	300	60	59
FeMn-MOF/NF(1:1)	NF	290(η_{50})	/	87.02	60
2D MOF-Fe/Co(1:2)	GCE	285(η_{50})	/	52	61
NiFe-BTC/CCHH/NF	NF	270(η_{50})	/	/	62
BN-CoFe-MOF	NF	314(η_{50})	/	105.6	63
$Ni_{0.6}Co_{1.8}$-MOF	NF	380(η_{200})	/	46	64
$Co_{0.8}Ni_{0.2}$Fc-MOF	GE	252(η_{200})	/	39	65

CFC: carbon fiber cloth; FF: Fe foam; CC: carbon cloth; GF: graphite foil; GE: graphite electrode

Table S3. Performance comparison of MOF-based electrolyzers in 1.0 M KOH.

Electrolyzers	Substrate	Cell voltage (V@10 mA cm^{-2})	Operation time (h)	Ref.
CeNiFe-MOF	NF	1.56	200	This work
NiFe-MOF-5	NF	1.57	24	6
NiFe(dobpdc)/NF	NF	1.59	30	7
Fe-Co-Ni MOF	NF	1.60	150	8
LIA-Ni-BDC|| LIA-MIL-101(Fe)	NF	1.59	50	12
CdFe-BDC	NF	1.63	12	13
BP@MOF	GCE	1.63	10	14
Fe_2V-MOF||Pt/C	NF	1.60	12	15
Co-MOF/NF	NF	1.548	24	16
VFe-MOF@NF	NF	1.61	1	17
CoFe-MOF@Pa	NF	1.66	36	18
NiFe-MOF/$NiSe_x$/NF	NF	1.59	40	23
Ni@CoO@Co-MOFC	NF	1.61	24	24
FeCoMnNi-MOF-74/NF	NF	1.62	30	26
ZnFe-BDC-0.75||Pt/C	NF	1.64	/	40
FeMn-MOF/NF(1:1)	NF	1.7@50	12	60
NiFe-BTC/CCHH/NF|| P-CCHH/NF	NF	1.55	12	62
dye@MOF	NF	1.98@35	4	66
NFF-MOF	NFF	1.57	24	67
NiFe-MOF array	NF	1.55	100	68
NiFe-MS/MOF@NF	NF	1.61	27	69
Ru@CoNi-MOF	NF	1.58@20	20	70
FeDy@MOF-Ni/CC||Pt/C	CC	1.57	80	71

NFF: NiFe foam

Table S4. Comparison of HER performance of the advanced electrocatalysts in alkaline seawater electrolyte.

Electrocatalysts	Substrate	η_{10} (mV)	Tafel slope (mV dec^{-1})	Ref.
CeNiFe-MOF		136	63.2	This
YNiFe-MOF	NF	155	73.4	work
LaNiFe-MOF		154	68.3	
Ni-SA/NC	NF	139	123	72
NiFe LDH/FeOOH	INF	181.8	/	73
Ni-Co@Fe-Co PBA	GCE	183	60	74
Ti@NiB	Ti plate	149	118	75
NRAHM-NiO	NF	178	115	76
CoP_x	NF	117	71.1	77
$(Co,Fe)PO_4$	IF	137	/	78
Mo-CoP_x/NF	NF	158	/	79
Co_xP_y/Ni_xP_y-NPC	GCE	203	135	80
Co-N,P-HCS	NF	164	109	81
$CoSe_2$-NCF	CC	134	67	82
$CoSe/MoSe_2$	GCE	189	/	83
1D-Cu@Co-CoO/Rh	CF	137.7	124.8	84
2D meso-Mo_2C/Mo_2N	GCE	197	67.6	85
Co@NCNT/$CoMo_yO_x$	CFP	125	/	86
Oct_Cu_2O-NF	NF	237(η_{20})	160	87
FMCO/NF	NF	250(η_{50})	/	88

INF: iron-nickel foam; IF: iron foam; CF: copper foam; CFP: carbon fiber paper

Table S5. Comparison of OER performance of the advanced electrocatalysts in alkaline seawater electrolyte.

Electrocatalysts	Substrate	η_{100} (mV)	η_{500} (mV)	Tafel slope (mV dec^{-1})	Ref.
CeNiFe-MOF		224	277	58.2	This
YNiFe-MOF	NF	243	273	46.6	work
LaNiFe-MOF		242	288	57.8	
Ni-BDC/NM88B(Fe)	NF	299	/	66.8	29
NiFe-MOF@NiS/NF	NF	296	355	86.2	34
NiFe-LDH/MOF	NF	307	/	61	39
ZnFe-BDC-0.75	NF	308	/	/	40
HMIL-88@PPy-TA	NF	259	345	53.7	57
$Ni_{0.6}Co_{1.8}$-MOF	NF	360	/	53	64
NiFe LDH/FeOOH	INF	286.2	/	/	73
NRAHM-NiO	NF	340	680	82	76
CoP_x@FeOOH	NF	283	337	50.3	77
Co-N,P-HCS	NF	490	/	121.5	81
NiIr-LDH	NF	315	361	78.8	89
NF/NiFe LDH	NF	247	296	/	90
NiFe-LDH-6-4/CC	CC	301	/	/	91
NiFe LDH-CeW@NFF	NFF	/	330	81.2	92
Ni_2Fe-LDH/$FeNi_2S_4$/NF	NF	271	/	/	93
S-$NiMoO_4$@NiFe-LDH	NF	315	/	/	94
$MnCo_2O_4$@NiFe-LDH/NF	NF	245	578	/	95
B-Co_2Fe LDH	NF	310	376	63.8	96
S-(Ni,Fe)OOH	NF	300	398	/	97
$FeOOH_{0.60}$/$Ni(HCO_3)_2$	CFP	324	/	/	98
FeOOH@2.5$Ni(OH)_2$/NF	NF	325	/	/	99
Fe-NiSOH	NF	263	311	/	100
NiPS/NF	NF	344	392	/	101
NiFeS/NF	NF	226	300	/	102
NiCoS/NF	NF	360	440	/	103
Cr-Co_xP	NF	334	392	/	104
MnCo/NiSe	NF	/	419.4	81.2	105
Mo-Ni_3S_2/NF	NF	291	/	/	106
Ni_2P-Fe_2P/NF	NF	305	/	/	107
Ni_3FeN@C/NF	NF	314	394	/	108
Ni_3S_2/Fe-NiP_x/NF	NF	290	336	61.3	109
$Ni(OH)_2$-TCNQ/GP	GP	382	/	75	110
NiCoHPi@Ni_3N/NF	NF	396	474	108.6	111
Mn-doped Ni_2P/Fe_2P	NF	270	325	/	112
B-$MnFe_2O_4$@MFOC	NF	405	/	/	113
MoS_2-$(FeNi)_9S_8$/NFF	NFF	256	/	/	114
Fe_2P/$Ni_{1.5}Co_{1.5}N$/Ni_2P	NF	255	307	/	115

GP: graphite paper

Table S6. Performance comparison of the advanced alkaline seawater electrolyzers.

Electrolyzers	Substrate	Cell voltage (V@10 mA cm^{-2})	Operation time (h)	Ref.
CeNiFe-MOF	NF	1.59	515	This work
CdFe-BDC	NF	1.68	/	13
Ru@CoNi-MOF	NF	1.67@20	18	70
Ni-Co@Fe-CoPBA|| NiCo@A-NiCo-PBA-AA	GCE	1.6@30	100	74
Ti@NiB	Ti plate	1.75@20	40	75
NiFeOOH//(Co,Fe)PO_4	IF	1.625	50	78
Mo-CoP_X/NF	NF	1.61	100	79
Co-N,P-HCS	NF	2.0@50	500	81
CoSe/$MoSe_2$/NF	NF	1.77	38	83
1D-Cu@Co-CoO/Rh	CF	1.70	12	84
Oct_Cu_2O-NF	NF	1.71	/	87
FMCO/NF	NF	1.59	180	88
$MnCo_2O_4$@NiFe-LDH	NF	1.56	100	95
$FeOOH_{0.60}$/$Ni(HCO_3)_2$||Pt/C	CFP	1.56	12	98
FeOOH@2.5$Ni(OH)_2$/NF|| Pt/C/NF	NF	1.63@20	72	99
Mn-doped Ni_2P/Fe_2P	NF	1.64	120	112
NiMo films	NF	1.62	18	116
CoF-3||CoF-2	CFP	1.76	≈20	117
PtO_x-NiO_n/NF	NF	1.58	/	118
FCNP@CQDs/CP	CP	1.61	50	119
Ni_{SA}-Ni_{Pi}/MoS_2 NSs	CC	1.66	15	120

References

1 G. Kresse and J. Furthmüller, *Comput. Mater. Sci.*, 1996, **6**, 15-50.

2 G. Kresse and J. Furthmuller, *Phys. Rev. B*, 1996, **54**, 11169-11186.

3 J. P. Perdew, K. Burke and M. Ernzerhof, *Phys. Rev. Lett.*, 1996, **77**, 3865-3868.

4 G. Kresse and D. Joubert, *Phys. Rev. B*, 1999, **59**, 1758-1775.

5 P. E. Blöchl, *Phys. Rev. B*, 1994, **50**, 17953-17979.

6 Q. X. Mou, Z. H. Xu, G. N. Wang, E. L. Li, J. Y. Liu, P. P. Zhao, X. H. Liu, H. B. Li and G. Z. Cheng, *Inorg. Chem. Front.*, 2021, **8**, 2889-2899.

7 L. X. Qi, Y. Q. Su, Z. C. Xu, G. H. Zhang, K. Liu, M. Liu, E. J. M. Hensen and R. Y. Y. Lin, *J. Mater. Chem. A*, 2020, **8**, 22974-22982.

8 F. S. Farahani, M. S. Rahmanifar, A. Noori, M. F. El-Kady, N. Hassani, M. Neek-Amal, R. B. Kaner and M. F. Mousavi, *J. Am. Chem. Soc*, 2022, **144**, 3411-3428.

9 F. J. Li, M. H. Jiang, C. G. Lai, H. F. Xu, K. Y. Zhang and Z. Jin, *Nano Lett.*, 2022, **22**, 7238-7245.

10 W. R. Cheng, H. B. Zhang, D. Y. Luan and X. W. Lou, *Sci. Adv.*, 2021, **7**, eabg2580.

11 F. P. Cheng, X. Y. Peng, L. Z. Hu, B. Yang, Z. J. Li, C. L. Dong, E. L. Chen, L. C. Hsu, L. C. Lei, Q. Zheng, M. Qiu, L. M. Dai and Y. Hou, *Nat. Commun.*, 2022, **13**, 6486.

12 Y. J. Tang, H. Zheng, Y. Wang, W. Zhang and K. Zhou, *Adv. Funct. Mater.*, 2021, **31**, 2102648.

13 Y. Luo, X. D. Yang, L. He, Y. Zheng, J. X. Pang, L. P. Wang, R. Jiang, J. Hou, X. H. Guo and L. Chen, *ACS Appl. Mater. Interfaces*, 2022, **14**, 46374-46385.

14 K. Ge, Y. Zhang, Y. Zhao, Z. H. Zhang, S. Wang, J. Y. Cao, Y. F. Yang, S. J. Sun, M. W. Pan and L. Zhu, *ACS Appl. Mater. Interfaces*, 2022, **14**, 31502-31509.

15 Y. X. Kong, D. K. Xiong, C. X. Lu, J. Wang, T. Liu, S. L. Ying, X. H. Ma and F. Y. Yi, *ACS Appl. Mater. Interfaces*, 2022, **14**, 37804-37813.

16 Z. Q. Huang, L. Hao, X. X. Ma, S. H. Zhang, R. Zhang, K. F. Yue and Y. Y. Wang, *Inorg. Chem.*, 2021, **60**, 4047-4057.

17 L. Han, J. Xu, Y. Huang, W. J. Dong and X. L. Jia, *Chin. Chem. Lett.*, 2021, **32**, 2263-2268.

18 T. Zhao, D. Z. Zhong, G. Y. Hao and Q. Zhao, *Appl. Surf. Sci.*, 2023, **607**, 155079.

19 S. Y. Dai, Y. Q. Liu, Y. J. Mei, J. Hu, K. M. Wang, Y. H. Li, N. H. Jin, X. Y. Wang, H. L. Luo and W. Li, *Dalton Trans.*, 2022, **51**, 15446-15457.

20 Q. Qiu, T. Wang, L. H. Jing, K. Huang and D. B. Qin, *Int. J. Hydrogen Energy*, 2020, **45**, 11077-11088.

21 W. H. Zhang, B. Q. Zhang, Y. A. Li, E. Z. Zhang, Y. Zhang, Q. Wang and Y. Q. Cong, *Int. J. Hydrogen Energy*, 2022, **47**, 1633-1643.

22 S. Li, H. Chai, L. Zhang, Y. Xu, Y. Jiao and J. Chen, *J. Colloid Interface Sci.*, 2023, **642**, 235-245.

23 S. X. Xu, J. Du, J. Y. Li, L. C. Sun and F. Li, *J. Mater. Chem. A*, 2020, **8**,

16908-16912.
24 Y. R. Wang, A. N. Wang, Z. Z. Xue, L. Wang, X. Y. Li and G. M. Wang, *J. Mater. Chem. A*, 2021, **9**, 22597-22602.
25 M. Fiaz and M. Athar, *Catal. Lett.*, 2020, **150**, 3314-3326.
26 M. Y. Zhang, W. Xu, T. T. Li, H. L. Zhu and Y. Q. Zheng, *Inorg. Chem.*, 2020, **59**, 15467-15477.
27 Y. S. Chen, J. K. Wang, Z. B. Yu, Y. P. Hou, R. H. Jiang, M. Wang, J. Huang, J. H. Chen, Y. Q. Zhang and H. X. Zhu, *Appl. Catal., B*, 2022, **307**, 121151.
28 T. T. Wang, Y. Wu, Y. Han, P. W. Xu, Y. J. Pang, X. Z. Feng, H. Yang, W. J. Ji and T. Cheng, *ACS Appl. Nano Mater.*, 2021, **4**, 14161-14168.
29 Y. Bao, H. Ru, Y. Wang, K. Zhang, R. Yu, Q. Wu, A. Yu, D. S. Li, C. Sun and W. Li, *Adv. Funct. Mater.*, 2024, **34**, 2314611.
30 J. Liang, X. T. Gao, B. Guo, Y. Ding, J. W. Yan, Z. X. Guo, E. C. M. Tse and J. X. Liu, *Angew. Chem., Int. Ed.*, 2021, **60**, 12770-12774.
31 J. Ding, D. Guo, N. Wang, H.-F. Wang, X. Yang, K. Shen, L. Chen and Y. Li, *Angew. Chem., Int. Ed.*, 2023, **62**, e202311909.
32 J. Zhou, Z. K. Han, X. K. Wang, H. Y. Gai, Z. K. Chen, T. Guo, X. B. A. Hou, L. L. Xu, X. J. Hu, M. H. Huang, S. V. Levchenko and H. Q. Jiang, *Adv. Funct. Mater.*, 2021, **31**, 2102066.
33 Y. Wang, B. R. Liu, X. J. Shen, H. Arandiyan, T. W. Zhao, Y. B. Li, M. Garbrecht, Z. Su, L. Han, A. Tricoli and C. Zhao, *Adv. Energy Mater.*, 2021, **11**, 2003759.
34 X. Hou, C. Yu, T. Ni, S. Zhang, J. Zhou, S. Dai, L. Chu and M. Huang, *Chin. J. Catal.*, 2024, **61**, 192-204.
35 Y. Z. Liu, X. T. Li, Q. D. Sun, Z. L. Wang, W. H. Huang, X. Y. Guo, Z. X. Fan, R. Q. Ye, Y. Zhu, C. C. Chueh, C. L. Chen and Z. L. Zhu, *Small*, 2022, **18**, 2201076.
36 Y. T. Jia, Z. K. Xu, L. Li and S. Y. Lin, *Dalton Trans.*, 2022, **51**, 5053-5060.
37 X. Sun, X. X. Zhang, Y. L. Li, Y. Z. Xu, H. Su, W. Che, J. F. He, H. Zhang, M. H. Liu, W. L. Zhou, W. R. Cheng and Q. H. Liu, *Small Methods*, 2021, **5**, 2100573.
38 C. P. Wang, Y. Feng, H. Sun, Y. R. Wang, J. Yin, Z. P. Yao, X. H. Bu and J. Zhu, *ACS Catal.*, 2021, **11**, 7132-7143.
39 M. Xiao, C. Wu, J. Zhu, C. Zhang, Y. Li, J. Lyu, W. Zeng, H. Li, L. Chen and S. Mu, *Nano Res.*, 2023, **16**, 8945-8952.
40 Y. K. Cheng, Y. Luo, Y. Zheng, J. X. Pang, K. S. Sun, J. Hou, G. Wang, W. Guo, X. H. Guo and L. Chen, *Int. J. Hydrogen Energy*, 2022, **47**, 35655-35665.
41 C. Li, W. Zhang, Y. Cao, J.-Y. Ji, Z.-C. Li, X. Han, H. Gu, P. Braunstein and J.-P. Lang, *Adv. Sci.*, 2024, **11**, 2401780.
42 Y. Ma, G. M. Mu, Y. J. Miao, D. M. Lin, C. G. Xu, F. Y. Xie and W. Zeng, *Rare Met.*, 2022, **41**, 844-850.
43 H. Qin, J. Cheng, P. Zhou, Z. Ji, H. Peng, X. Shen, H. Zhou, G. Zhu and J. Yang, *Chem. Eng. J.*, 2024, **493**, 152721.
44 D. K. Xiong, M. L. Gu, C. Chen, C. X. Lu, F. Y. Yi and X. H. Ma, *Chem. Eng.*

J., 2021, **404**, 127111.
45 Y. Liu, X. Li, S. Zhang, Z. Wang, Q. Wang, Y. He, W. H. Huang, Q. Sun, X. Zhong, J. Hu, X. Guo, Q. Lin, Z. Li, Y. Zhu, C. C. Chueh, C. L. Chen, Z. Xu and Z. Zhu, *Adv. Mater.*, 2023, **35**, 2300945.
46 Z. Y. Zhao, X. X. Sun, H. W. Gu, Z. Niu, P. Braunstein and J. P. Lang, *ACS Appl. Mater. Interfaces*, 2022, **14**, 15133-15140.
47 C. F. Li, L. J. Xie, J. W. Zhao, L. F. Gu, H. B. Tang, L. Zheng and G. R. Li, *Angew. Chem., Int. Ed.*, 2022, **61**, e202116934.
48 F. P. Cheng, Z. J. Li, L. Wang, B. Yang, J. G. Lu, L. C. Lei, T. Y. Ma and Y. Hou, *Mater. Horiz.*, 2021, **8**, 556-564.
49 D. Y. Liu, Z. F. Zhao, Z. K. Xu, L. Li and S. Y. Lin, *Dalton Trans.*, 2022, **51**, 12839-12847.
50 N. K. Shrestha, S. A. Patil, S. Cho, Y. Jo, H. Kim and H. Im, *J. Mater. Chem. A*, 2020, **8**, 24408-24418.
51 S. Pavithra, V. K. Jothi, A. Rajaram, S. Ingavale and A. Natarajan, *Energy Fuels*, 2022, **36**, 6409-6419.
52 Y. Li, Y. Zhang, Z. Wang, C. Zhang, F. Meng, J. Zhao, X. Li and J. Hu, *Appl. Catal., A*, 2024, **683**, 119851.
53 C. X. Zhang, Q. L. Qi, Y. J. Mei, J. Hu, M. Z. Sun, Y. J. Zhang, B. L. Huang, L. B. Zhang and S. H. Yang, *Adv. Mater.*, 2023, **35**, 2208904.
54 A. Sikdar, A. Majumdar, A. Gogoi, P. Dutta, M. Borah, S. Maiti, C. Gogoi, K. A. Reddy, Y. Oh and U. N. Maiti, *J. Mater. Chem. A*, 2021, **9**, 7640-7649.
55 Y. Wang, S. Wang, Z. L. Ma, L. T. Yan, X. B. Zhao, Y. Y. Xue, J. M. Huo, X. Yuan, S. N. Li and Q. G. Zhai, *Adv. Mater.*, 2022, **34**, 2107488.
56 H. Yin, X. Liu, L. Wang, T. T. Isimjan, D. Cai and X. Yang, *Inorg. Chem.*, 2024, **63**, 7045-7052.
57 Y. X. Chen, L. Shen, C. C. Wang, S. Y. Feng, N. Zhang, K. Zhang and B. Yang, *Chem. Eng. J.*, 2022, **430**, 132632.
58 Q.-N. Bian, B.-S. Guo, D.-X. Tan, D. Zhang, W.-Q. Kong, C.-B. Wang and Y.-Y. Feng, *ACS Appl. Mater. Interfaces*, 2024, **16**, 14742-14749.
59 X. J. Zhai, Q. P. Yu, G. S. Liu, J. L. Bi, Y. Zhang, J. Q. Chi, J. P. Lai, B. Yang and L. Wang, *J. Mater. Chem. A*, 2021, **9**, 27424-27433.
60 H. X. Guan, N. Wang, X. X. Feng, S. K. Bian, W. Li and Y. Chen, *Colloids Surf. A*, 2021, **624**, 126596.
61 K. Ge, S. J. Sun, Y. Zhao, K. Yang, S. Wang, Z. H. Zhang, J. Y. Cao, Y. F. Yang, Y. Zhang, M. W. Pan and L. Zhu, *Angew. Chem., Int. Ed.*, 2021, **60**, 12097-12102.
62 N. N. Ma, C. Q. Fei, J. Wang and Y. L. Wang, *J. Alloys Compd.*, 2022, **917**, 165511.
63 L. Shen, X. Zhang, H. He, X. Fan, W. Peng and Y. Li, *J. Colloid Interface Sci.*, 2024, **676**, 238-248.
64 S. Shang, W. Li, L. Zhang, S. Liu, Q. Tang, Y. Ding, C. Li, Y. Sun and H. Wu, *Chem. Eng. J.*, 2024, **496**, 154093.
65 J. S. Hu, Q. L. Xu, X. Y. Wang, X. H. Huang, C. H. Zhou, Y. Ye, L. Zhang and

H. Pang, *Carbon Energy*, 2023, **5**, e315.
66 C. Jiao, M. Hu, T. Hu and J. Zhang, *J. Solid State Chem.*, 2023, **322**, 123978.
67 W. X. Chen, X. W. Zhu, Y. W. Zhang, Y. M. Zhou and K. K. Ostrikov, *ACS Sustain. Chem. Eng.*, 2021, **9**, 1826-1836.
68 Y. T. Sun, S. Ding, S. S. Xu, J. J. Duan and S. Chen, *J. Power Sources*, 2021, **494**, 229733.
69 M. Zhao, W. Li, J. Y. Li, W. H. Hu and C. M. Li, *Adv. Sci.*, 2020, **7**, 2001965.
70 W. Li, B. Guo, K. Zhang, X. Chen, H. Zhang, W. Chen, H. Chen, H. Li and X. Feng, *J. Colloid Interface Sci.*, 2024, **668**, 181-189.
71 Z. X. Wan, Q. T. He, J. D. Chen, T. T. Isimjan, B. Wang and X. L. Yang, *Chin. J. Catal.*, 2020, **41**, 1745-1753.
72 W. J. Zang, T. Sun, T. Yang, S. B. Xi, M. Waqar, Z. K. Kou, Z. Y. Lyu, Y. P. Feng, J. Wang and S. J. Pennycook, *Adv. Mater.*, 2021, **33**, 2003846.
73 K. Jiang, W. J. Liu, W. Lai, M. L. Wang, Q. Li, Z. L. Wang, J. J. Yuan, Y. L. Deng, J. Bao and H. B. Ji, *Inorg. Chem.*, 2021, **60**, 17371-17378.
74 H. Zhang, J. F. Diao, M. Z. Ouyang, H. Yadegari, M. X. Mao, M. N. Wang, G. Henkelman, F. Xie and D. J. Riley, *ACS Catal.*, 2023, **13**, 1349-1358.
75 Y. R. Zhang, C. Y. Fu, J. L. Fan, H. Y. Lv and W. J. Hao, *J. Electroanal. Chem.*, 2021, **901**, 115761.
76 K. Hemmati, A. Kumar, A. R. Jadhav, O. Moradlou, A. Z. Moshfegh and H. Lee, *ACS Catal.*, 2023, **13**, 5516-5528.
77 L. B. Wu, L. Yu, B. McElhenny, X. X. Xing, D. Luo, F. H. Zhang, J. M. Bao, S. Chen and Z. F. Ren, *Appl. Catal., B*, 2021, **294**, 120256.
78 C. Kim, S. Lee, S. H. Kim, J. Park, S. Kim, S. H. Kwon, J. S. Bae, Y. S. Park and Y. Kim, *Nanomaterials*, 2021, **11**, 2989.
79 Y. Yu, J. Li, J. Luo, Z. Kang, C. Jia, Z. Liu, W. Huang, Q. Chen, P. Deng, Y. Shen and X. Tian, *Mater. Today Nano*, 2022, **18**, 100216.
80 L. Zhu, Y. H. Huang, B. L. Wang, Y. Zhang, R. Y. Zou, L. J. Yan and W. Sun, *J. Solid State Electrochem.*, 2022, **26**, 233-243.
81 X. K. Wang, X. K. Zhou, C. Li, H. X. Yao, C. H. Zhang, J. Zhou, R. Xu, L. Chu, H. L. Wang, M. Gu, H. Q. Jiang and M. H. Huang, *Adv. Mater.*, 2022, **34**, 2204021.
82 H. H. Chen, S. S. Zhang, Q. Liu, P. Yu, J. Luo, G. Z. Hu and X. J. Liu, *Inorg. Chem. Commun.*, 2022, **146**, 110170.
83 J. P. Sun, J. Li, Z. Z. Li, C. H. Li, G. M. Ren, Z. S. Zhang and X. C. Meng, *ACS Sustain. Chem. Eng.*, 2022, **10**, 9980-9990.
84 P. K. L. Tran, D. T. Tran, D. Malhotra, S. Prabhakaran, D. Kim, N. H. Kim and J. H. Lee, *Small*, 2021, **17**, 2103826.
85 S. Li, Z. Y. Zhao, T. Ma, P. Pachfule and A. Thomas, *Angew. Chem., Int. Ed.*, 2022, **61**, e202112298.
86 Q. Quan, X. M. Bu, D. Chen, F. Wang, X. L. Kang, W. Wang, Y. Meng, S. Yip, C. T. Liu and J. C. Ho, *J. Mater. Chem. A*, 2022, **10**, 3953-3962.
87 H. Wang, J. Ying, Y. X. Xiao, J. B. Chen, J. H. Li, Z. Z. He, H. J. Yang and X. Y. Yang, *Electrochem. Commun.*, 2022, **134**, 107177.

88 W. Liu, W. Que, R. Yin, J. Dai, D. Zheng, J. Feng, X. Xu, F. Wu, W. Shi, X. Liu and X. Cao, *Appl. Catal., B*, 2023, **328**, 122488.
89 H. H. You, D. S. Wu, D. H. Si, M. N. Cao, F. F. Sun, H. Zhang, H. M. Wang, T. F. Liu and R. Cao, *J. Am. Chem. Soc*, 2022, **144**, 9254-9263.
90 M. Ning, L. Wu, F. Zhang, D. Wang, S. Song, T. Tong, J. Bao, S. Chen, L. Yu and Z. Ren, *Mater. Today Phys.*, 2021, **19**, 100419.
91 G. F. Dong, F. Y. Xie, F. X. Kou, T. T. Chen, F. Y. Wang, Y. W. Zhou, K. C. Wu, S. W. Du, M. Fang and J. C. Ho, *Mater. Today Energy*, 2021, **22**, 100883.
92 M. Li, H.-J. Niu, Y. Li, J. Liu, X. Yang, Y. Lv, K. Chen and W. Zhou, *Appl. Catal., B*, 2023, **330**, 122612.
93 L. Tan, J. T. Yu, C. Wang, H. F. Wang, X. E. Liu, H. T. Gao, L. T. Xin, D. Z. Liu, W. G. Hou and T. R. Zhan, *Adv. Funct. Mater.*, 2022, **32**, 2200951.
94 H. Y. Wang, L. Y. Chen, L. Tan, X. E. Liu, Y. H. Wen, W. G. Hou and T. R. Zhan, *J. Colloid Interface Sci.*, 2022, **613**, 349-358.
95 N. Kitiphatpiboon, M. Chen, C. R. Feng, Y. F. Zhou, C. L. Liu, Z. B. Feng, Q. Zhao, A. Abudula and G. Q. Guan, *J. Colloid Interface Sci.*, 2023, **632**, 54-64.
96 L. B. Wu, L. Yu, Q. C. Zhu, B. McElhenny, F. H. Zhang, C. Z. Wu, X. X. Xing, J. M. Bao, S. Chen and Z. F. Ren, *Nano Energy*, 2021, **83**, 105838.
97 L. Yu, L. B. Wu, B. McElhenny, S. W. Song, D. Luo, F. H. Zhang, Y. Yu, S. Chen and Z. F. Ren, *Energy Environ. Sci.*, 2020, **13**, 3439-3446.
98 M. H. Lin, Y. Yang, Y. H. Song, D. G. Guo, L. P. Yang and L. Liu, *Nano Res.*, 2023, **16**, 2094-2101.
99 Y. Yang, M. H. Lin, Y. H. Song, G. Tuerhong, J. Q. Dai, T. Zhang, D. G. Guo and L. Liu, *J. Alloys Compd.*, 2022, **910**, 164879.
100 C. Q. Huang, Q. C. Zhou, D. S. Duan, L. Yu, W. Zhang, Z. Z. Wang, J. Liu, B. W. Peng, P. F. An, J. Zhang, L. P. Li, J. G. Yu and Y. Yu, *Energy Environ. Sci.*, 2022, **15**, 4647-4658.
101 H. Y. Wang, J. T. Ren, L. Wang, M. L. Sun, H. M. Yang, X. W. Lv and Z. Y. Yuan, *J. Energy Chem.*, 2022, **75**, 66-73.
102 J. Chen, L. C. Zhang, J. Li, X. He, Y. Y. Zheng, S. J. Sun, X. D. Fang, D. D. Zheng, Y. S. Luo, Y. Wang, J. Zhang, L. S. Xie, Z. W. Cai, Y. T. Sun, A. A. Alshehri, Q. Q. Kong, C. W. Tang and X. P. Sun, *J. Mater. Chem. A*, 2023, **11**, 1116-1122.
103 C. Z. Wang, M. Zhu, Z. Cao, P. Zhu, Y. Cao, X. Y. Xu, C. Xu and Z. Y. Yin, *Appl. Catal., B*, 2021, **291**, 120071.
104 Y. Song, M. Sun, S. Zhang, X. Zhang, P. Yi, J. Liu, B. Huang, M. Huang and L. Zhang, *Adv. Funct. Mater.*, 2023, **33**, 2214081.
105 R. Andaveh, A. Sabour Rouhaghdam, J. Ai, M. Maleki, K. Wang, A. Seif, G. Barati Darband and J. Li, *Appl. Catal., B*, 2023, **325**, 122355.
106 C. Lan, H. P. Xie, Y. F. Wu, B. Chen and T. Liu, *Energy Fuels*, 2022, **36**, 2910-2917.
107 L. B. Wu, L. Yu, F. H. Zhang, B. McElhenny, D. Luo, A. Karim, S. Chen and Z. F. Ren, *Adv. Funct. Mater.*, 2021, **31**, 2006484.
108 B. R. Wang, M. J. Lu, D. Chen, Q. Zhang, W. W. Wang, Y. T. Kang, Z. X. Fang,

G. S. Pang and S. H. Feng, *J. Mater. Chem. A*, 2021, **9**, 13562-13569.
109 X. Luo, P. X. Ji, P. Y. Wang, X. Tan, L. Chen and S. C. Mu, *Adv. Sci.*, 2022, **9**, 2104846.
110 L. C. Zhang, J. Q. Wang, P. Y. Liu, J. Liang, Y. S. Luo, G. W. Cui, B. Tang, Q. Liu, X. D. Yan, H. G. Hao, M. L. Liu, R. Gao and X. P. Sun, *Nano Res.*, 2022, **15**, 6084-6090.
111 H. Sun, J. K. Sun, Y. Y. Song, Y. F. Zhang, Y. Qiu, M. X. Sun, X. Y. Tian, C. Y. Li, Z. Lv and L. X. Zhang, *ACS Appl. Mater. Interfaces*, 2022, **14**, 22061-22070.
112 Y. Z. Luo, P. Wang, G. X. Zhang, S. S. Wu, Z. S. Chen, H. Ranganathan, S. H. Sun and Z. C. Shi, *Chem. Eng. J.*, 2023, **454**, 140061.
113 M. Chen, N. Kitiphatpiboon, C. Feng, Q. Zhao, A. Abudula, Y. Ma, K. Yan and G. Guan, *Appl. Catal., B*, 2023, **330**, 122577.
114 S. W. Song, Y. H. Wang, S. Y. Zhou, H. W. Gao, X. Q. Tian, Y. G. Yuan, W. Li and J. B. Zang, *ACS Appl. Energy Mater.*, 2022, **5**, 1810-1821.
115 F. M. Zhang, Y. L. Liu, F. Yu, H. J. Pang, X. Zhou, D. Y. Li, W. Q. Ma, Q. Zhou, Y. X. Mo and H. Q. Zhou, *ACS Nano*, 2023, **17**, 1681-1692.
116 W. J. Yuan, Z. D. Cui, S. L. Zhu, Z. Y. Li, S. L. Wu and Y. Q. Liang, *Electrochim. Acta*, 2021, **365**, 137366.
117 B. Debnath, S. Parvin, H. Dixit and S. Bhattacharyya, *ChemSusChem*, 2020, **13**, 3875-3886.
118 W. L. Yu, H. R. Liu, Y. Zhao, Y. L. Fu, W. P. Xiao, B. Dong, Z. X. Wu, Y. M. Chai and L. Wang, *Nano Res.*, 2023, **16**, 6517-6530.
119 S. Lv, Y. Deng, Q. Liu, Z. Fu, X. Liu, M. Wang, Z. Xiao, B. Li and L. Wang, *Appl. Catal., B*, 2023, **326**, 122403.
120 M. S. Kim, D. T. Tran, T. H. Nguyen, V. A. Dinh, N. H. Kim and J. H. Lee, *Energy Environ. Mater.*, 2022, **5**, 1340-1349.